

# Observations of the Eruptions of July 22 and August 7, 1980, at Mount St. Helens, Washington

---

U.S. GEOLOGICAL SURVEY PROFESSIONAL PAPER 1335



COVER—Mount St. Helens as viewed from the north on July 22, 1980, showing the formation of a pyroclastic density flow. Photograph by Harry X. Glicken.

**OBSERVATIONS OF THE ERUPTIONS  
OF JULY 22 AND AUGUST 7, 1980,  
AT MOUNT ST. HELENS, WASHINGTON**

FRONTISPIECE—Mount St. Helens as viewed from the north at about 1906 PDT, during the second of the three eruptive pulses of July 22, 1980. The vertical-eruption column is derived directly from the vent, whereas the ash cloud rising through the atmospheric clouds in the foreground is derived from a pyroclastic density flow. Tephra can be seen falling from the left side of the vertical column. Mount Hood, Oreg., is visible in the background. Photograph by James W. Vallance.







# Observations of the Eruptions of July 22 and August 7, 1980, at Mount St. Helens, Washington

By RICHARD P. HOBLITT

---

U.S. GEOLOGICAL SURVEY PROFESSIONAL PAPER 1335

*A description and discussion of pyroclastic density flows  
and other eruptive phenomena*



**DEPARTMENT OF THE INTERIOR**

**DONALD PAUL HODEL, *Secretary***

**U.S. GEOLOGICAL SURVEY**

**Dallas L. Peck, *Director***

**Library of Congress Cataloging in Publication Data**

Hoblitt, Richard P.

Observations of the eruptions of July 22 and August 7, 1980, at Mount St. Helens, Washington  
(Geological Survey Professional Paper ; 1335)

Bibliography: p.

Supt. of Docs. No.: I 19.16:1335

1. Saint Helens, Mount (Wash.)—Eruption, 1980.

I. Title. II. Series.

QE523.S23H63 1985

551.2'1'0979784

84-600141

---

For sale by the Superintendent of Documents,  
U.S. Government Printing Office  
Washington, D.C. 20402

## CONTENTS

	Page		Page
Abstract	1	Discussion—Continued	
Introduction	1	Speculations concerning a relief-valve mechanism	32
Acknowledgments	2	Features associated with the front of the pyroclastic density flow formed by the third eruptive pulse of July 22, 1980	34
Terminology	2	Temperatures of the pyroclastic-flow deposits of July 22, 1980	35
Crater geometry	3	A possible genetic relationship between pyroclastic flows and pyroclastic surges during the eruption of August 7, 1980	35
Eruptions of July 22, 1980	4	References cited	38
Eruption of August 7, 1980	15	Appendix.—Determination of the velocity of the pyroclastic density flow	42
Emplacement data for pyroclastic flows of July 22 and August 7, 1980	20		
Discussion	20		
The eruptions of July 22 and August 7, 1980, in comparison with other eruptions	20		
The eruptions of July 22 and August 7, 1980, in terms of column-collapse models	21		

## ILLUSTRATIONS

	Page
FRONTISPICE. Mount St. Helens as viewed from the north at about 1906 PDT, during the second eruptive pulse of July 22, 1980.	
FIGURE 1. Index map of the Mount St. Helens region	2
2. Topographic map of the area around the crater, dome, and north flank of Mount St. Helens, from photographs taken on July 1, 1980	3
3-10. Photographs showing:	
3. Amphitheater as viewed from the north at about 1800 PDT on July 22, 1980, between first and second eruptive pulses	5
4. Mount St. Helens as viewed from the north, sequence showing about the first 30 s of the second eruptive pulse of July 22, 1980	6
5. Mount St. Helens as viewed from the northwest at about 1826:17 PDT on July 22, 1980, about 1 min after the beginning of the second eruptive pulse	12
6. Mount St. Helens as viewed from the northwest at about 1826:30 PDT on July 22, 1980	13
7. Mount St. Helens as viewed from the west-southwest, second eruptive pulse between 1830 and 1831 PDT on July 22, 1980	14
8. Amphitheater as viewed from the north at about 1859 PDT on July 22, 1980, moderate level of activity about 1 min before start of third eruptive pulse	16
9. Amphitheater as viewed from the north on July 22, 1980, sequence of the early part of the third eruptive pulse	17
10. Amphitheater as viewed from the north at 1916:48 PDT on July 22, 1980, vertical column with helical form	21
11. Topographic maps of area around the vent of Mount St. Helens, from photographs taken on July 1 and July 31, 1980	22
12. Photographs showing Mount St. Helens as viewed from Coldwater Peak on August 7, 1980, sequence of the early part of the first eruptive pulse	23
13. Graph showing velocity of the flow front as a function of distance from the vent for the flow observed on August 7, 1980	29
14. Photograph showing Mount St. Helens as viewed from the north on August 15, 1980, and path of pyroclastic density flow of August 7, 1980	30
15. Topographic map of area around the path of the flow of August 7, 1980, from photographs taken on September 6, 1980	31
16-19. Diagrams showing:	
16. Hypothetical relief-valve mechanism	33
17. Two alternative solutions for the flow field in the host medium of a density flow	35
18. Mechanism that may have operated during the flow observed on August 7, 1980	37
19. Procedure used to extract flow-front positions from photographs	42
20. Diagrammatic topographic map illustrating construction of average vertical profile through flow path	43
21. Diagrammatic vertical profile through average flow path	44

TABLE

---

	Page
TABLE 1. Emplacement data for pyroclastic flows of July 22 and August 7, 1980, compared to previously reported emplacement data for small and large pyroclastic flows .....	20

# OBSERVATIONS OF THE ERUPTIONS OF JULY 22 AND AUGUST 7, 1980, AT MOUNT ST. HELENS, WASHINGTON

By RICHARD P. HOBLITT

## ABSTRACT

The explosive eruptions of July 22 and August 7, 1980, at Mount St. Helens, Wash., both included multiple eruptive pulses. The beginnings of three of the pulses—two on July 22 and one on August 7—were witnessed and photographed. Each of these three began with a fountain of gases and pyroclasts that collapsed around the vent and generated a pyroclastic density flow. Significant vertical-eruption columns developed only after the density flows were generated. This behavior is attributable to either an increase in the gas content of the eruption jet or a decrease in vent radius with time. An increase in the gas content may have occurred as the vent was cleared (by expulsion of a plug of pyroclasts) or as the eruption began to tap deeper, gas-rich magma after first expelling the upper, gas-depleted part of the magma body. An effective decrease of the vent radius with time may have occurred as the eruption originated from progressively deeper levels in the vent. All of these processes—vent clearing; tapping of deeper, gas-rich magma; and effective decrease in vent radius—probably operated to some extent. A “relief-valve” mechanism is proposed here to account for the occurrence of multiple eruptive pulses. This mechanism requires that the conduit above the magma body be filled with a bed of pyroclasts, and that the vesiculation rate in the magma body be inadequate to sustain continuous eruption. During a repose interval, vesiculation of the magma body would cause gas to flow upward through the bed of pyroclasts. If the rate at which the magma produced gas exceeded the rate at which gas escaped to the atmosphere, the vertical pressure difference across the bed of pyroclastic debris would increase, as would the gas-flow rate. Eventually a gas-flow rate would be achieved that would suddenly diminish the ability of the bed to maintain a pressure difference between the magma body and the atmosphere. The bed of pyroclasts would then be expelled (that is, the relief valve would open) and an eruption would commence. During the eruption, gas would be lost faster than it could be replaced by vesiculation, so the gas-flow rate in the conduit would decrease. Eventually the gas-flow rate would decrease to a value that would be inadequate to expel pyroclasts, so the conduit would again become choked with pyroclasts (that is, the relief valve would close). Another period of repose would commence. The eruption/repose sequence would be repeated until gas-production rates were inadequate to reopen the valve, either because the depth of the pyroclast bed had become too great, the volatile content of the magma had become too low, or the magma had been expended.

A timed sequence of photographs of a pyroclastic density flow on August 7 indicates that, in general, the velocity of the flow front was determined by the underlying topography. Observations and details of the velocity/topography relationship suggest that both pyroclastic flows and pyroclastic surges formed. The following mechanism is consistent with the data. During initial fountain collapse and when the

flow passed over steep, irregular terrain, a highly inflated suspension of gases and pyroclasts formed. In this suspension, the pyroclasts underwent rapid differential settling according to size and density; a relatively low-concentration, fine-grained upper phase formed over a relatively high-concentration coarse-grained phase. The low-particle-concentration phase (the pyroclastic surge) was subject to lower internal friction than the basal high-concentration phase (the pyroclastic flow), and so accelerated away from it. The surge advanced until it had deposited so much of its solid fraction that its net density became less than that of the ambient air. At this point it rose convectively off the ground, quickly decelerated, and was overtaken by the pyroclastic flow.

The behavior of the flow of August 7 suggests that a pyroclastic density flow probably expands through the ingestion of air wherever it passes over surfaces whose relief is a significant fraction of the flow thickness. Thus, a pyroclastic flow may spawn one or more pyroclastic surges at locations remote from the source volcano. The ingestion of air by a pyroclastic surge would increase the time that particles would be held in suspension and, thus, extend the lifetime and length of the pyroclastic surge.

## INTRODUCTION

The reawakening of Mount St. Helens (fig. 1) offered an unusual opportunity to document the rarely observed, short-lived phenomena that occur during explosive eruptions. An early explosive phase of activity was defined by the magmatic eruptions of May 18, May 25, June 12, July 22, August 7, and October 16–18, 1980. Of these, the eruptions of July 22 and August 7 were, at least with regard to flowage phenomena, the most closely observed and photographically best documented.<sup>1</sup> This report presents some observations and photographs of eruption phenomena that occurred on July 22 and August 7, and suggests mechanisms to explain them. The emphasis is on the pulsating nature of the eruptions, the timing of pyroclastic density flow formation relative to vertical-eruption column development, and the generation and motion of pyroclastic

<sup>1</sup>These two eruptions were also monitored by radar. For details of column heights and ash content deduced by this method see Harris and others (1980, 1981).

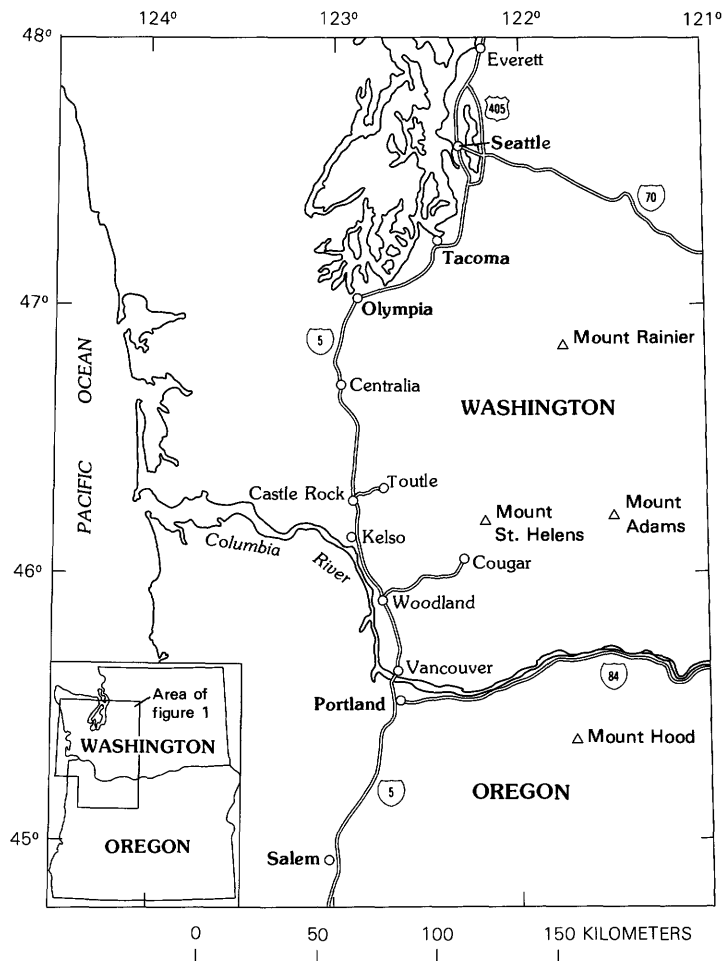


FIGURE 1.—Index map of the Mount St. Helens region.

flows and surges. Also considered are the emplacement temperatures of pyroclastic-flow deposits, and phenomena probably related to the displacement of air by an advancing pyroclastic density flow.

### ACKNOWLEDGMENTS

The U.S. Forest Service staff at Gifford Pinchot National Forest helped provide communications and logistic support for this study. Their efforts and those of the University of Washington/U.S. Geological Survey seismic-monitoring team are sincerely appreciated. Michael Montgomery skillfully piloted our helicopter, sometimes in demanding circumstances, during the eruptions of both July 22 and August 7. I am indebted to Janis Markman for efficiently carrying out the duties of helicopter dispatcher at all hours of the day and night. Many of the photographs presented in this report, or referred to in its preparation, were taken by

others. I wish to thank J. W. Vallance, C. D. Miller, H. X. Glicken, M. P. Doukas, L. A. McBroome, T. J. Bornhorst, Terry Leighley, P. W. Lipman, and R. D. Denslinger for making their photographs available to me. One of the topographic maps used in this report was kindly prepared by D. E. Fair. The artwork for many of the illustrations was provided by Barbara M. Myers. Useful discussions and criticisms of the manuscript were provided by W. Z. Savage, D. R. Crandell, W. E. Scott, D. R. Mullineaux, R. V. Fisher, J. W. Vallance, and R. S. J. Sparks.

### TERMINOLOGY

A bewildering variety of names has been applied to the types of flowage phenomena that are described in this report. The same is true of the resulting deposits. Here, the term pyroclastic flow is used to mean a hot, dry density flow of gases and volcanic rock debris whose



density is similar to the density of the resulting deposit. The deposit is termed a pyroclastic-flow deposit. The term pyroclastic surge is used here to mean a hot, dry density flow of gases and volcanic rock debris whose density is much less than that of the resulting deposit, which is called a pyroclastic-surge deposit. When used without a modifier, "flow" is used as a synonym for pyroclastic density flow; that is, as a nonspecific term for pyroclastic flow or pyroclastic surge.

## CRATER GEOMETRY

The paroxysmal events of May 18, 1980—failure of the north side of the mountain, the resultant directed blast, and subsequent plinian eruption (Christiansen and Peterson, 1981)—produced a deep crater breached to the north; this crater, U-shaped in plan, will be referred to as the amphitheater. A vent was situated at the center of the crater floor (fig. 2). Prior to July 22, a

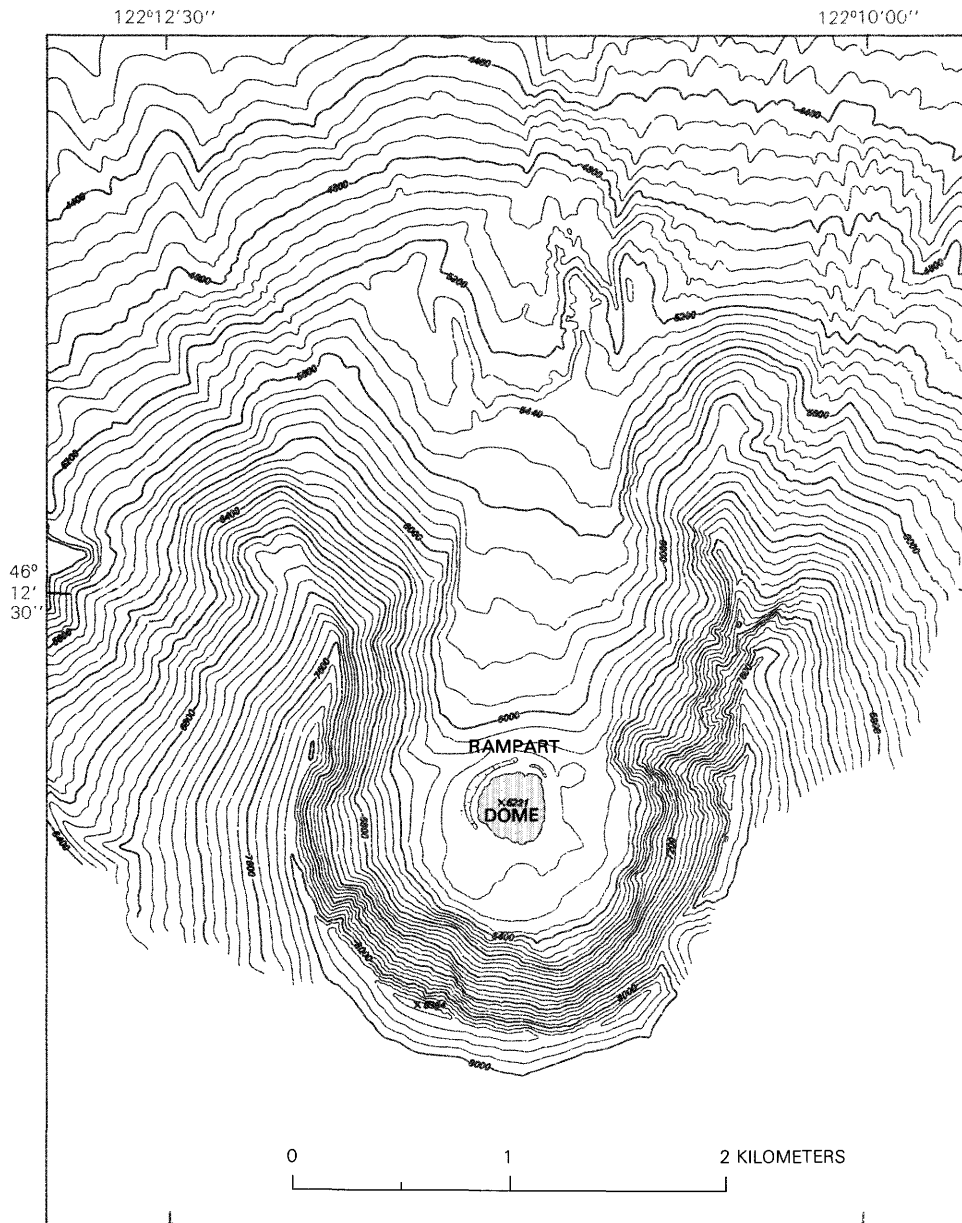


FIGURE 2.—Topographic map of the area around the crater, dome (shaded), and north flank of Mount St. Helens, prepared from photographs (USGS) taken on July 1, 1980. Contours and elevations in feet; hachures indicate areas of topographic lows; 1 ft = 0.3048 m.

circularly symmetric dome, whose diameter was about 325 m and whose maximum exposed thickness was about 45 m, lay centered over the vent (fig. 2). This mass was extruded after the explosive eruption of June 12 (Moore and others, 1981). A low, semicircular rampart of ejecta spanned the crater breach north of the dome (fig. 2). The rampart was roughly concentric to, and about 250 m from, the dome center.

It is interesting to note that Mount Lamington, Papua New Guinea, a volcano whose 1951–52 eruptive sequence rather closely parallels the 1980–81 eruptions at Mount St. Helens, had a crater geometry similar to that described above, including a breach-spanning rampart, at a correlative stage in the eruptive activity (Taylor, 1958, p. 59).

### ERUPTIONS OF JULY 22, 1980

On July 22, the beginning of the first of three eruptive pulses was reported at 1714 PDT by U.S. Forest Service observer Richard D. Denslinger from a fixed-wing aircraft (unpub. records of the Gifford Pinchot National Forest). Although U.S. Geological Survey field parties were working near Mount St. Helens at the time of the eruption, the north side of the mountain was largely obscured from ground observation by a cloud layer. I first observed and photographed the eruption through broken clouds from a helicopter to the west of the mountain at 1719 PDT. An unobstructed view just above the cloud tops at 1722 PDT gave no indication that a pyroclastic flow or surge had occurred. However, a set of seven untimed eruption photographs taken by Denslinger from the northeast indicates otherwise. Denslinger's sequence probably begins within 2 min of the onset of the eruption. This is several minutes before I had a clear view. In addition to a voluminous, vertical-eruption plume, his photographs show ash clouds rising convectively from the amphitheater floor. This indicates that at least one density flow was produced by the first eruptive pulse. Because of obscuring atmospheric clouds, the northward limit of the ash clouds cannot be located accurately, but it certainly did not exceed 2 km from the vent. Thus, compared to the density flows produced by the succeeding eruptive pulses, this flow was small. Denslinger's photographs do not include the beginning of the eruption, so the timing of flow formation relative to the onset of eruption is uncertain. However, it is clear that the flow formed early and might have formed at the beginning of the eruption.

The vigor of the eruption column waned quickly (noticeably by 1719 PDT), and by 1732 the voluminous, light-gray, ash-laden clouds of the early eruption had been replaced by much less voluminous white steam

clouds. As the level of activity declined, visibility within the amphitheater improved, so at 1757 PDT we flew past the mouth of the amphitheater to observe the effects of the eruption. The floor of the amphitheater appeared to be covered with new pyroclastic-flow deposits. The northern part of the dome was still intact but, as evidenced by the source of the steam clouds, it had been disrupted somewhere between its center and southern margin (fig. 3). At 1808 PDT Denslinger reported that the center portion of the dome was missing<sup>2</sup> (unpub. records of the Gifford Pinchot National Forest).

At 1814 PDT, it was necessary to leave the mountain to refuel the helicopter; consequently, I was not present for the start of the second eruptive pulse.

When the second eruptive pulse commenced at 1825 PDT, visibility in the vicinity of the vent was good. The eruption was photographed until 1831 by James W. Vallance from a U.S. Forest Service fixed-wing aircraft. Vallance's photographs show that the pulse began with the appearance of a dark (ash-rich), colloform eruption cloud (fig. 4A). Within 30 s the expanding cloud filled the entire amphitheater (figs. 4A–J). However, it showed little tendency to develop vertically; rather, colloform ash clouds rose convectively from a fountaining suspension of gases and pyroclasts (figs. 4C–J). Projections of this "pyroclastic fountain" followed trajectories with maximum heights of as much as (approximately) 800 m above the vent. (A projection is indicated with an arrow on fig. 4H.) A growing pyroclastic density flow was apparently initiated and fed by the projections as they collided with the amphitheater floor. The flow front is discernible on figures 4C and 4D, but is best displayed on succeeding photographs of the sequence, after the front emerges from the shadow obscuring the amphitheater floor. (The flow front is indicated with a dashed line on fig. 4H.) The flow front was initially unembayed (or embayed on a fine scale) and roughly semicircular in plan; the leading portion was centered on the amphitheater floor (figs. 4D–F). When the flow front reached a point about 1 km north of the ejecta rampart, it became increasingly digitate with three well-defined lobes at the center flanked by two or three others that were less well formed (figs. 4G–J). About 30 s after the start of the eruption, the flow front passed from view beneath the atmospheric clouds. The mean velocity to this point—about 1.2 km north of the vent—was about 40 m/s. Although the flow was now hidden from view, its progress was marked by convecting ash clouds that rose from it and penetrated the atmospheric cloud layer. About 1 min after the start of the pulse, a vertical-

<sup>2</sup>After the eruptions of July 22, breadcrust bombs, some weighing more than 50 kg, were found about 1.5 km northwest of the vent. These were probably fragments of the central part of the dome that was explosively disrupted at the outset of the first eruptive pulse.



FIGURE 3.—Amphitheater as viewed from the north at about 1800 PDT on July 22, 1980, between the first and second eruptive pulses. Northern part of the dome (arrow) is visible above rampart (dashed line). Mild steam clouds emanate from the center of the dome. Distance from dome center to base of crater wall is about 0.5 km. (Photograph by Michael P. Doukas.)

eruption column began to form rapidly. Figure 5 shows the eruption clouds as viewed from the northwest about 1 min after the pulse began. The mean rise velocity of the cloud top during the first minute was about 60 m/s. By the time an additional 13 s had elapsed, the appearance of the eruption clouds had changed dramatically (fig. 6). The mean rise velocity of that part of the cloud directly above the vent during these 13 s was about 130 m/s. On figure 6, the ash cloud rising from the pyroclastic flow and the vertical column can not be differentiated on the basis of color. However, within about 5 min (fig. 7) the vertical column became distinctly darker, apparently because it carried a greater proportion of ash. This suggests that fragmental material was then being fed preferentially into the vertical column rather than being fed to the density flow.

When I returned to the north side of the mountain at 1853 PDT, the ash cloud from the pyroclastic density flow had dissipated and the amphitheater was again clear. The eruption had waned but the level of activity was, both in terms of the ash content and emission rate of the plume, greater than that observed during the lull

between the first and second eruptive pulses. This moderate level of activity persisted until a third (final) eruptive pulse began.

A few minutes before 1900 PDT, we began an east-to-west helicopter traverse about 4.5 km north of the amphitheater, which afforded a good view of the dome and vent (fig. 8). The surface of the dome, which appeared dark colored and rough after the first pulse, appeared light colored and smooth after the second pulse. Its general profile remained unchanged; evidently, the chief effect of the second pulse on the dome was to mantle its surface with a thin layer of ejecta.

At about 1900 PDT, the moderate ash emission gave way to a vertical to subvertical fountain of "spearhead" ash projections (Taylor, 1958, p. 32). These projections—shaped like long, thin, inverted V's—rose perhaps as much as 100 m above the crater floor before the ejecta that composed them fell back into the vent. The overall appearance of this activity was suggestive of a great (albeit overactivated) fluidized bed. The height of the fountain then began to increase noticeably. Within 10 s of the time that this increase first became

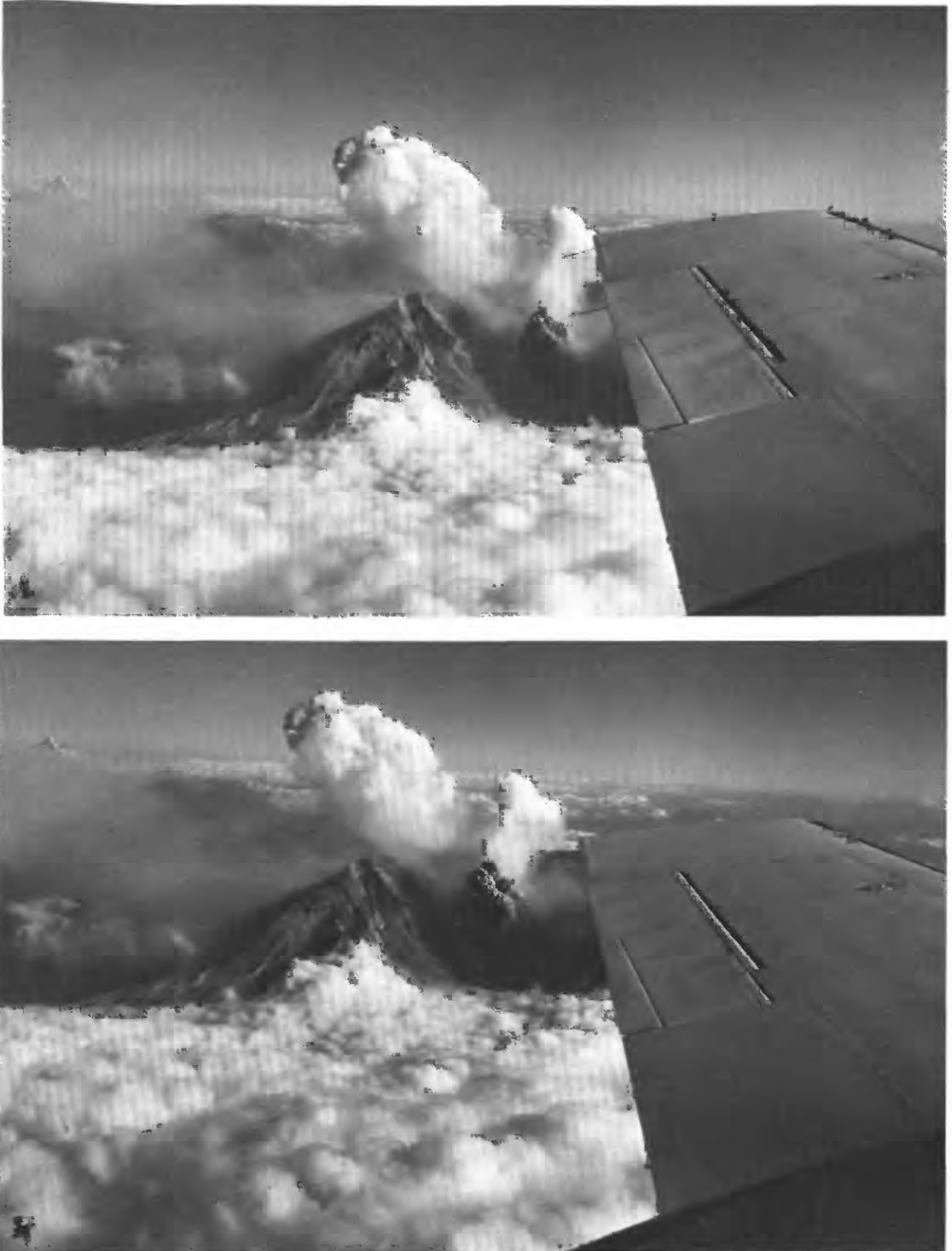


FIGURE 4.—Mount St. Helens as viewed from the north, sequence (4A–J) showing about the first 30 s of the second eruptive pulse of July 22, 1980. Photographs 4A–I taken at about 3-s intervals beginning at 1825:20±5 PDT; photograph 4J taken about 6 s



after 4I. Arrow (4H) indicates projection from pyroclastic fountain. Dashed line (4H) indicates front of pyroclastic density flow. (Photographs by James W. Vallance.)



FIGURE 4.—Continued



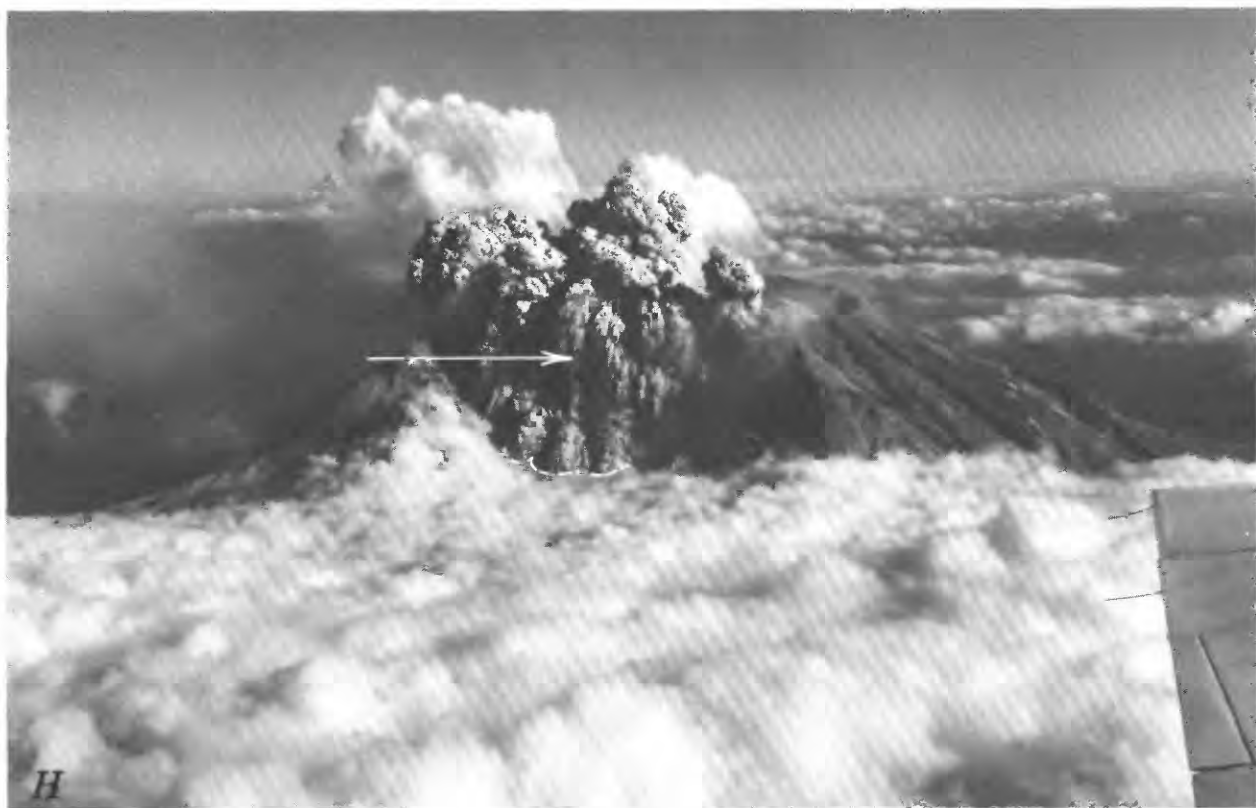


FIGURE 4.—Continued



FIGURE 4.—Continued

apparent, the fountain rose to about 400 m above the crater floor and ejecta began to fall outside the vent. A small pyroclastic density flow immediately appeared as it began to spill over the rampart (fig. 9A). I recorded the first 9 s of flowage with a clock-equipped camera; subsequent photographs (taken by H. X. Glicken) were not timed. The photographs clearly show (figs. 9B-D) that the flow was derived from the fountain: it originated from areas where the trajectories of projections intersected the floor and walls of the amphitheater. Four seconds after the flow began (fig. 9B), its leading point was about 150 m north of the ejecta rampart. In general, the flow was parabolic in plan, with a width of about 300 m at the ejecta rampart. In detail, the flow margins exhibited lobe-and-cleft structures (Simpson, 1969; Allen, 1971a; Fisher, 1977); lobes ranged in width from about 10 m to a few tens of meters. As it advanced northward, the flow maintained a rough bilateral symmetry about the axis of the amphitheater. Nine seconds after the flow began, the front was about 250 m north of the rampart. The flow was no longer parabolic in plan as the leading part had become rather blunt (fig. 9C); it advanced along an east-west-trending front about 500 m wide. Within another five seconds<sup>3</sup> the front had advanced to about 400 m north of the rampart, and a

distinct large-scale cleft had appeared at the center of the flow front (fig. 9D). This cleft divided the front more or less symmetrically into two lobes, each about 300 m across. Each of these, in turn, was divided into two poorly defined secondary lobes. These secondary lobes were somewhat better defined by the time the front was about 750 m north of the rampart (fig. 9E). Until this point, the flow had maintained a rough bilateral symmetry about the axis of the amphitheater. About 1 km north of the rampart, however, the flow became asymmetrical as the front advanced with shifting, irregular embayments (fig. 9F). At this point the flow, which had been expanding laterally as it advanced, had completely covered the amphitheater floor and had begun to move up the amphitheater walls. The flow reached a height of about 200 m above the amphitheater floor on the west wall and a somewhat lower height on the east wall. Perhaps the complex flow-front geometry was due to the influence of the walls on the flow.

Because of our flight path, our view of the flow front was obscured beyond this point by the atmospheric cloud layer that shielded the north flank of the

<sup>3</sup>This is an estimate based on the assumption that flow velocities at the times of the untimed photographs were similar to those determined from the timed photographs.





FIGURE 4.—Continued

mountain.

Within a few seconds of our last observation, Vallance began to take photographs from the U.S. Forest Service aircraft that was now about 11 km west-northwest of the crater at an altitude of 5 km. At this time the flow front was emerging from the mouth of the amphitheater, roughly 1.5 km north of the ejecta rampart. The front now consisted of four or five lobes similar to those observed during the second eruptive pulse. The multiple lobes coalesced into two lobes about 1.6 km from the rampart. Evidently this was caused by the underlying topography, because at this point the gently sloping floor of the amphitheater merges northward with two

north-trending channels. After advancing an additional few hundred meters, the front became obscured as it passed beneath the clouds.

As it moved through the amphitheater, the flow front had a distinct overhang (best displayed on figs. 9C-E). For the first 10 to 15 s, this overhang was less pronounced at the flow nose, where it was 10 m thick or less, than on the flow flanks, where it was as much as several tens of meters thick. This difference seemed to diminish with time. For about the first kilometer of travel, the front was in the shadow of the west wall of the amphitheater. The overhang, manifest on the photographs as a dark band at the flow front, seemed to dis-

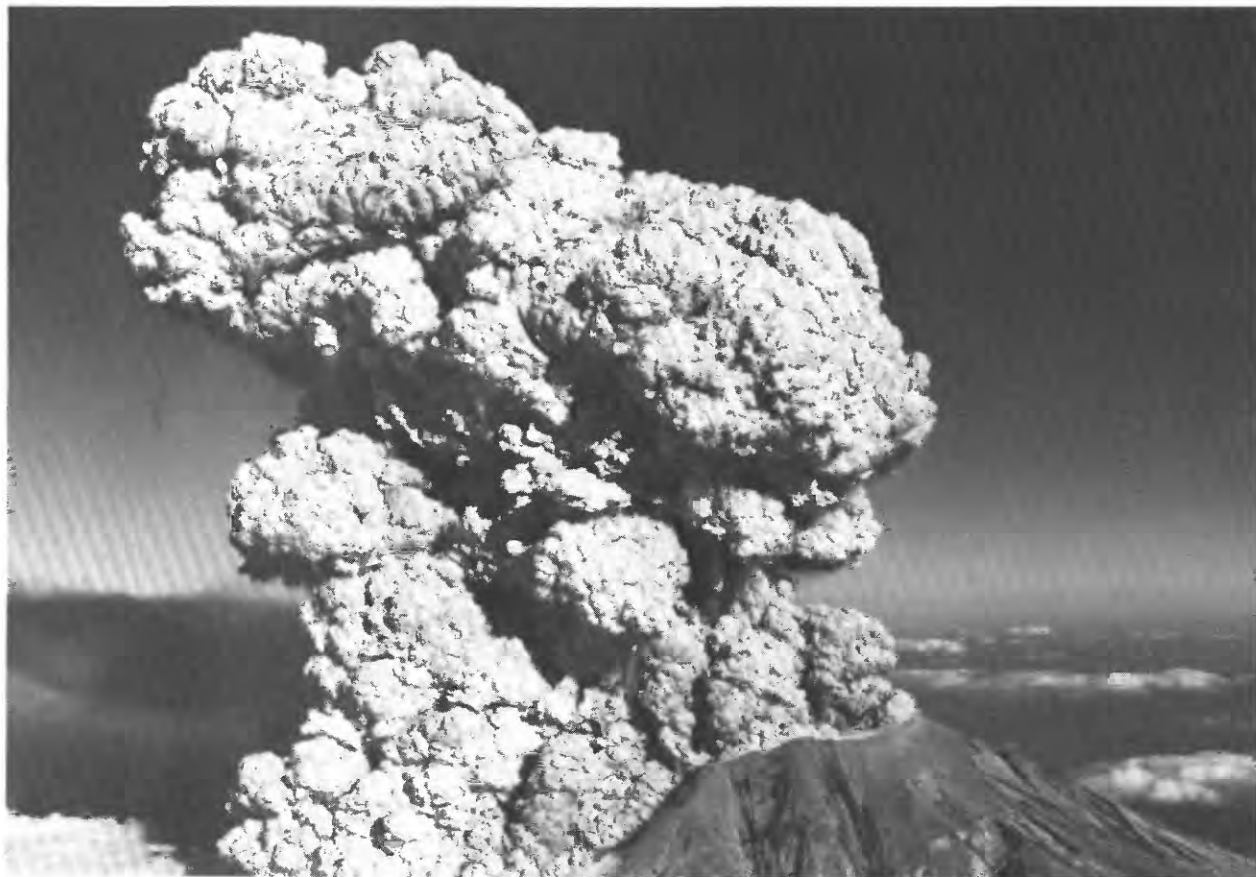


FIGURE 5.—Mount St. Helens as viewed from the northwest at about 1826:17 PDT on July 22, 1980, about 1 min after the beginning of the second eruptive pulse. Highest point on the eruption cloud is about 3,000 m above highest visible point on the rim of the amphitheater. (Photograph by James W. Vallance.)

appear as the flow moved from the shadow into direct sunlight, apparently due to the change in lighting conditions.

About 10 s after the flow first appeared, diffuse light-colored areas appeared on the amphitheater floor (fig. 9C). One of these adjoined the west side of the flow front, the others were between the west margin of the flow and the adjacent wall of the amphitheater. Within the next 5 s, the light-colored areas became more extensive. Now, the flow front was immediately preceded by, and in contact with, a diffuse, light-colored zone that in places exhibited striae or rays normal to the front (fig. 9D). The diffuse zone was, in turn, preceded by and merged into a series of discontinuous bands that paralleled the flow front. These bands are discernible in fig. 9D, but are best displayed in fig. 9E. The width of the region in which this phenomenon was most obvious was about 50 m, although isolated, faint bands could be seen within a few hundred meters of the flow front. In those areas where they were well developed, the width of the bands and the spacing between them was about 5–10 m.

The band thickness was probably no more than a few meters; the diffuse, light-colored zone along the flow front may have been somewhat thicker, particularly immediately adjacent to the front. Unfortunately, it was not possible to tell if the bands were moving or stationary. Once the flow front reached the mouth of the amphitheater and emerged from shadow into direct sunlight, the phenomenon was much less apparent.

A vertical-eruption column began to develop about 1/2 to 1 min after the third pulse began, at a time when the density flow was already well under way (compare figs. 9E–G). By 1915 PDT, the region near the vent, which had been obscured since the pyroclastic fountain appeared, cleared again and the eruption column could be seen rotating in a clockwise direction as it rose (fig. 10). Such rotation apparently is not unique, as a photograph of a 1951 eruption of Mount Lamington shows a similar feature (Taylor, 1958, fig. 32).

The effect of the third pulse on the dome was not observed until the day after the eruption. Remnants of the dome could clearly be seen in the walls of the vent.

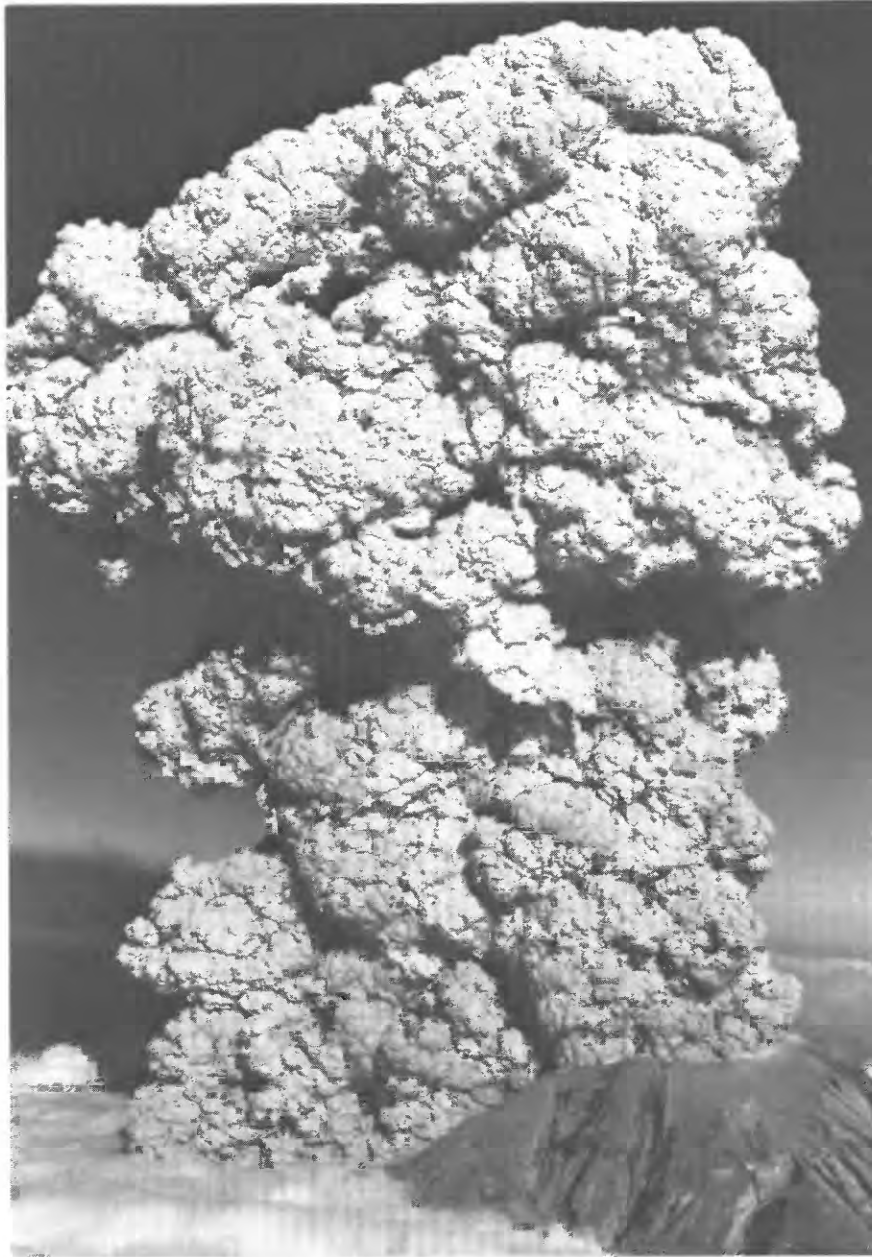


FIGURE 6.—Mount St. Helens as viewed from the northwest, showing the second eruptive pulse at about 1826:30 PDT on July 22, 1980, about 13 s after the view shown in figure 5. Note that (compare fig. 5) a vertical column is forming rapidly. Highest point on the eruption cloud is about 4,100 m above the highest visible point on the rim of the amphitheater. (Photograph by James W. Vallance.)

However, sufficient ejecta had accumulated around the vent to otherwise conceal the remnants. The topography of the vent area after the eruption of July 22 is shown in figure 11.

Two units are recognizable in the pyroclastic-flow deposits produced by the eruptions of July 22. (See Rowley and others, 1981; Kuntz and others, 1981, for

discussions of these deposits.) A lower, cream-colored unit is the more extensive of the two and apparently was emplaced by the pyroclastic flow of the second eruptive pulse, and an upper, salmon-colored unit is a product of the third pulse. Each unit consists of a 1- to 2-m-thick sheet of rounded dacite pumice blocks in an ash matrix; a small fraction of the blocks are bread-



FIGURE 7.—Mount St. Helens as viewed from the west-southwest, showing the second eruptive pulse between 1830 and 1831 PDT on July 22, 1980. Note that the vertical column is distinctly darker than the ash cloud rising from the pyroclastic density flow that is moving to the north beneath the atmospheric cloud layer. (Photograph by James W. Vallance.)

crusted. Margins of these deposits are lobate and have distinct levees and noses that have less ash than their central portions.

Emplacement-temperature data for these units are summarized by Banks and Hoblitt (1981). The lower deposit generally yielded lower emplacement temperatures than did the upper deposit. The maximum temperatures measured in the lower deposit were generally less than 600 °C, whereas the maximum temperatures of the upper deposit exceeded 600 °C. A temperature in excess of 600 °C was measured in the lower deposit on only one occasion; this was about 1 hr after emplacement, at a site on the flow margin. The surface here consisted almost entirely of pumice cobbles, but at depths of a few to a few tens of centimeters the interstices were filled with ash. I recorded the maximum temperature—about 660 °C—in the void space between the surface cobbles. Then, as the thermocouple probe was pushed down into the underlying ash matrix, the temperature began to fall (the magnitude of the decrease was not recorded). Apparently the ash was emplaced at a lower tempera-

ture than the pumice cobbles. Further evidence of an inhomogeneous emplacement-temperature distribution was obtained during the next few days when temperature probes were inserted into the deposits. Occasionally, a probe would be stopped by a large pumice block at some depth. The temperature of these blocks was greater than that of the finer grained debris that enclosed them.

Shortly after emplacement, the central portions of many pyroclastic-flow lobes exhibited a markedly fluid behavior. As a result, these areas were treacherous to walk on. It was common to sink 0.5 m or more into ash and pumice whose temperature exceeded 500 °C. The problem could generally be avoided by “patting” an area with one’s boot before placing full weight on it. This caused gases to escape from the fluid mass at numerous points around the disturbed area. Within a few seconds the area would “set up” and support a person’s full weight. (See Wilson and Head, 1981, for a discussion of flow rheology.) The fluid behavior of the deposits ceased, probably due to capillary phenomena,



after they had been wetted by rain. The levees and toes of the flow deposits were not fluid, even shortly after emplacement, presumably because of their high proportion of pumice blocks to ash matrix.

## ERUPTION OF AUGUST 7, 1980

The onset of harmonic tremor at 1217 PDT on August 7 suggested that an eruption was imminent (Malone and others, 1981). Observation from the ground was possible because of clear skies; consequently, we began an eruption watch from Coldwater Peak, a good vantage point about 11 km to the north of Mount St. Helens. However, visibility was hampered by windblown ash deflated from the amphitheater walls by low-altitude winds. Low-altitude winds blew to the northwest, whereas high-altitude winds blew to the northeast.

When we arrived at Coldwater Peak (at 1423 PDT), vent activity consisted of mild steam emissions. At 1438 PDT a dark (presumably ash-rich) plume rose to a height of about 300 m above the vent. By 1447 PDT this plume had apparently dissipated. By 1454 a second dark plume was visible; this appeared to reach about the same height as the first plume. For the next 1½ hours the plume height continued to fluctuate; the maximum plume height during this time was about 600 m above the vent (about level with the rim of the amphitheater).

The eruption began with the appearance of a white steam plume over the western part of the vent area at about 1623 PDT. The plume quickly grew into a vertical column; by 1626:12 the top of the column was about 3,500 m above the vent (fig. 12A). As the column grew, its lower portion became progressively darker and presumably increasingly rich in ash. The profile of the east side of the column, clearly visible from the vantage point of Coldwater Peak (fig. 12A), was essentially vertical. Shortly before 1627 PDT, the lower part of the vertical profile was rapidly replaced by crescentic projections (fig. 12B) resembling those of the pyroclastic fountains of July 22. This change was accompanied by a pronounced, low-frequency rumbling noise. The projections traversed the distance between the vent and east amphitheater wall (about 600 m) in about 8 s. The projection velocity, about 75 m/s, may approximate that of the ejection velocity. The growth of the initial vertical-eruption column stopped when the ash projections appeared. The ash cloud resulting from the initial vertical eruption became diffuse and began to drift north-northwest.

Within 10 s of the first appearance of the projections, the front of a pyroclastic density flow could be vaguely discerned through the haze as a faint, light-colored band

that stretched along the amphitheater floor from wall to wall. At this time, the flow front was about 1 km north of the vent. I photographed the flow at intervals of a few seconds to a few tens of seconds with a clock-equipped camera until forward movement terminated; examples are shown in figures 12C-L. These photographs allow mean velocities to be determined<sup>4</sup> at intervals along that part of the flow path over which the flow front is clearly visible (fig. 13). The front could first be clearly seen through the haze about 45 s after the ash projections appeared; at this time the front was about 1.3 km north of the center of the vent. The front advanced rapidly at first and then, about 1.7 km north of the vent center, seemed to stagnate (fig. 12C). About 1 min after the flow started, a vertical-eruption column—that became much larger than the initial column—began to develop over the vent.

The pyroclastic density flows of July 22 and August 7 followed two paths down the north flank of the volcano. The leading part of the flow of August 7 advanced out of the west side of the amphitheater and entered the head of the western path. The ash cloud rising from this western flow then cast a shadow on portions of the eastern path. Because of this, the eastern flow was only barely visible except when it moved into direct sunlight; the eastern flow will not be considered further.

The path followed by the leading part of the western flow is shown in profile in figure 13, in an oblique aerial view in figure 14, and in plan view in figure 15. At altitudes between about 1,500 and 1,180 m, the path coincided with a channel eroded by previous pyroclastic flows; this channel consisted of a series of alternating benches and cliffs that resembled stairsteps. The upper part of the channel, between altitudes of about 1,500 and 1,270 m, constituted the steepest segment of the path. At about 1,350 m, the channel changed course rather abruptly from due north to about 30° east of north. At 1,270 m, the mean slope of the steps decreased, and near 1,240 m the channel curved about 20° back toward the north. At 1,180 m, the mouth of the channel emptied onto the apex of the "pumice plain," a broad aggradational fan of pyroclastic-flow deposits.

Overall, the channel controlled the course of the flow; the nose followed it closely, whereas the body followed it generally. Once the nose passed a given point in the channel, the body of the flow expanded laterally beyond the confining channel walls. For example, 10 s after it began to descend the steep upper part of the channel, the flow extended as much as 100 m to either side (compare figs. 12E, F). At curves, the expanding body of the flow overrode the channel walls in a manner analogous

<sup>4</sup>The procedure used to determine flow velocities is given in the appendix.



FIGURE 8.—Amphitheater as viewed from the north at about 1859 PDT on July 22, 1980, showing moderate level of activity about 1 min before the start of the third eruptive pulse.

to a bobsled leaving a course at a sharp bend. The portion of the flow that overrode a curve then lost momentum and an ash cloud rose convectively from it. This behavior served to exaggerate the curves followed by the flow nose. As the flow front descended the steep parts of the path, its thickness appeared to decrease; at times it was about 10 m or perhaps less (fig. 12F).

Convectively rising ash clouds marked the progress of the flow; in general, the height and volume of the cloud rising above a given point on the path were directly related to the time elapsed since the front passed that point. The rate at which clouds of ash were produced varied along the path, thus the resulting aggregate cloud developed protuberances. Major protuberances emanated from along each of the two braced path segments shown in figures 14 and 15. The flow-front positions of figures 12D and 12E approximately delimit the path segment indicated by the lower brace. The delimiting photographs for the upper brace are shown in figures 12E and 12I. Each protuberance rose above a segment of the flow path over which the flow front accelerated and then decelerated. Bends in the flow path also seem to have affected the rate of ash-cloud production because significant contributions to the second

major protuberance originated from the bends at altitudes of 1,350 and 1,240 m.

The character of the flow front changed shortly after it moved onto the gently sloping pumice plain; the convex, colloform ash clouds (figs. 12H-I) rose off of the ground (fig. 12J) and were succeeded by a thin, light-colored wedge (figs. 12K-L). This change was synchronous with the velocity low that occurred on the pumice plain at about 1,150 m altitude (fig. 13, time interval 13). The leading part of the wedge was no more than a few meters thick. Following the change, the flow became digitate as distinct lobes advanced radially away from the apex of the aggradational fan. The advance then stopped about 6.5 min after the pyroclastic fountain initiated the flow. During this terminal phase, the rate of ash-cloud generation decreased markedly.

FIGURE 9 (facing page).—Amphitheater as viewed from the north on July 22, 1980, sequence (9A-G) showing the formation of a pyroclastic density flow during the early part of the third eruptive pulse. A, 1900:59; B, 1901:03 PDT, timed photographs by the author; C, 1901:08 PDT, photography by Harry X. Glicken, time from comparison with a timed photograph that is not shown; D, E, F, G, untimed sequence taken within 30 s after C, by Harry X. Glicken.

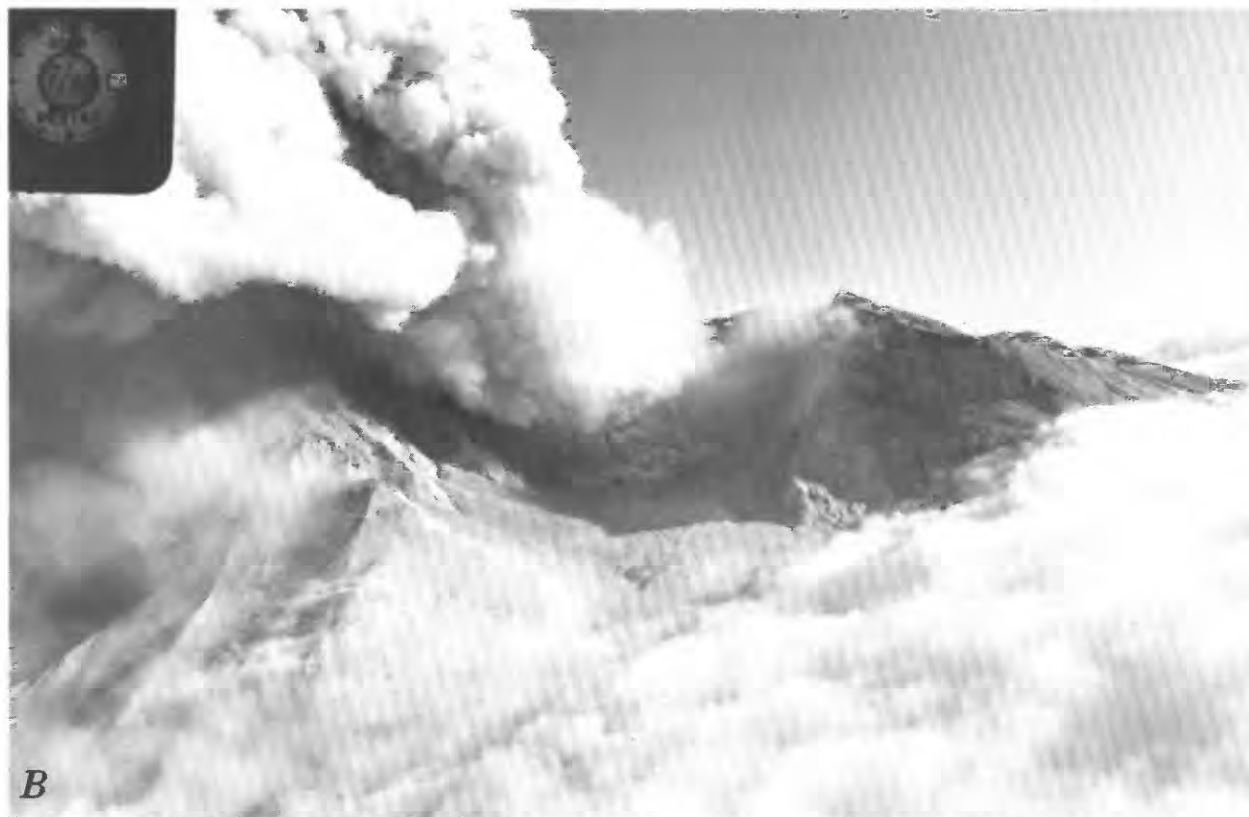




FIGURE 9.—Continued





FIGURE 9.—Continued



G

FIGURE 9.—Continued

About 10 min after the start of the eruption, a tephra curtain obscured the northwest to northeast sector of the mountain. Thus, although additional eruptive pulses occurred on August 7 (Harris and others, 1981; Malone and others, 1981), only the first was observed to emplace a pyroclastic flow. The distribution of the deposits of August 7 coincides with the observed geometry of the flow front at the time flowage stopped. Therefore, if any of the subsequent pulses produced flows—and field evidence suggests that at least one of them did—their deposits were less extensive than the deposit produced by the first pulse.

### EMPLACEMENT DATA FOR PYROCLASTIC FLOWS OF JULY 22 AND AUGUST 7, 1980

Emplacement data for the pyroclastic flows of July 22 and August 7 are compared with those of other pyroclastic flows (Sheridan, 1979) in table 1. This comparison indicates that the mobility of the Mount St. Helens flows approached that of much larger pyroclastic flows.

TABLE 1.—Emplacement data for pyroclastic flows of July 22 and August 7, 1980, compared to previously reported emplacement data for small and large pyroclastic flows

[Leaders (---), no data available]

Pyroclastic flow	Deposit slope (degrees)	Runout (L) (km)	Vertical drop (H) (km)	Fountain height (m)	H/L
July 22					
Second pulse -----	1.5	6.5	1.7	800	0.26
Third pulse -----	1.5	5.9	1.2	400	.20
August 7 -----	1.5	5.7	1.1-1.3	300-500	0.19-0.23
Small flows <sup>1</sup>					
Most mobile -----	2.4	15.0	4.5	3,000(?)	.30
Least mobile -----	25.	1.9	1.4	500	.74(?)
Large flows <sup>1</sup>					
Most mobile -----	.7	76.	---	---	.06
Least mobile -----	1.5	22.	---	---	.20

<sup>1</sup>From Sheridan, 1979.

### DISCUSSION

#### THE ERUPTIONS OF JULY 22 AND AUGUST 7, 1980, IN COMPARISON WITH OTHER ERUPTIONS

The literature contains accounts of eruptions apparently similar in behavior to those described earlier in this report. However, most accounts are insufficiently



FIGURE 10.—Amphitheater as viewed from the north at 1916:48 PDT on July 22, 1980, showing helical nature of vertical-eruption column that was visible once the ash cloud from the pyroclastic density flow shown on figure 9 dissipated.

detailed to make close comparisons. Perhaps the closest analog is given by Taylor (1958) in his description of “shallow pocket” explosions and resultant nuées ardentes that he witnessed during the 1951 eruptions of Mount Lamington, Papua New Guinea. Similar behavior was probably also exhibited by Mayon Volcano, Republic of the Philippines, in 1968 (Moore and Melson, 1969).

Nairn and Self (1978) described in detail the periodic, cannon-like explosions that generated pyroclastic avalanches during the eruptions of Ngauruhoe Volcano, New Zealand, in 1975. These were discrete events that commenced with visible shock waves. Within a few tenths of a second after the appearance of the shock wave, a slug of compressed gases and fragmental material was ejected, and began to expand in all directions. These shallow cannon-like explosions were probably similar to the first eruptive pulse of July 22, which explosively disrupted a plug dome. However, the cannon-like behavior contrasts to the pyroclastic fountaining observed at the outset of the second and third pulses of July 22 and the first pulse of August 7. The fountains

were more sustained events that increased in intensity over a period of many seconds. Each can be likened to a vertically directed garden hose whose water pressure is gradually increased. An additional difference is that the Mount St. Helens fountains gave way to vertical-eruption columns, whereas the Ngauruhoe explosions were separated by periods of quiescence.

#### THE ERUPTIONS OF JULY 22 AND AUGUST 7, 1980, IN TERMS OF COLUMN-COLLAPSE MODELS

In two observed cases on July 22, a pyroclastic fountain generated a pyroclastic density flow before a vertical-eruption column developed. The major vertical column observed on August 7 also developed after a pyroclastic fountain appeared, although the fountain was preceded by a minor vertical column.

It is useful to consider the fountains, flows, and subsequent vertical columns in terms of the column-collapse models of Sparks and Wilson (1976), Sparks and others (1978), and Wilson and others (1980). These



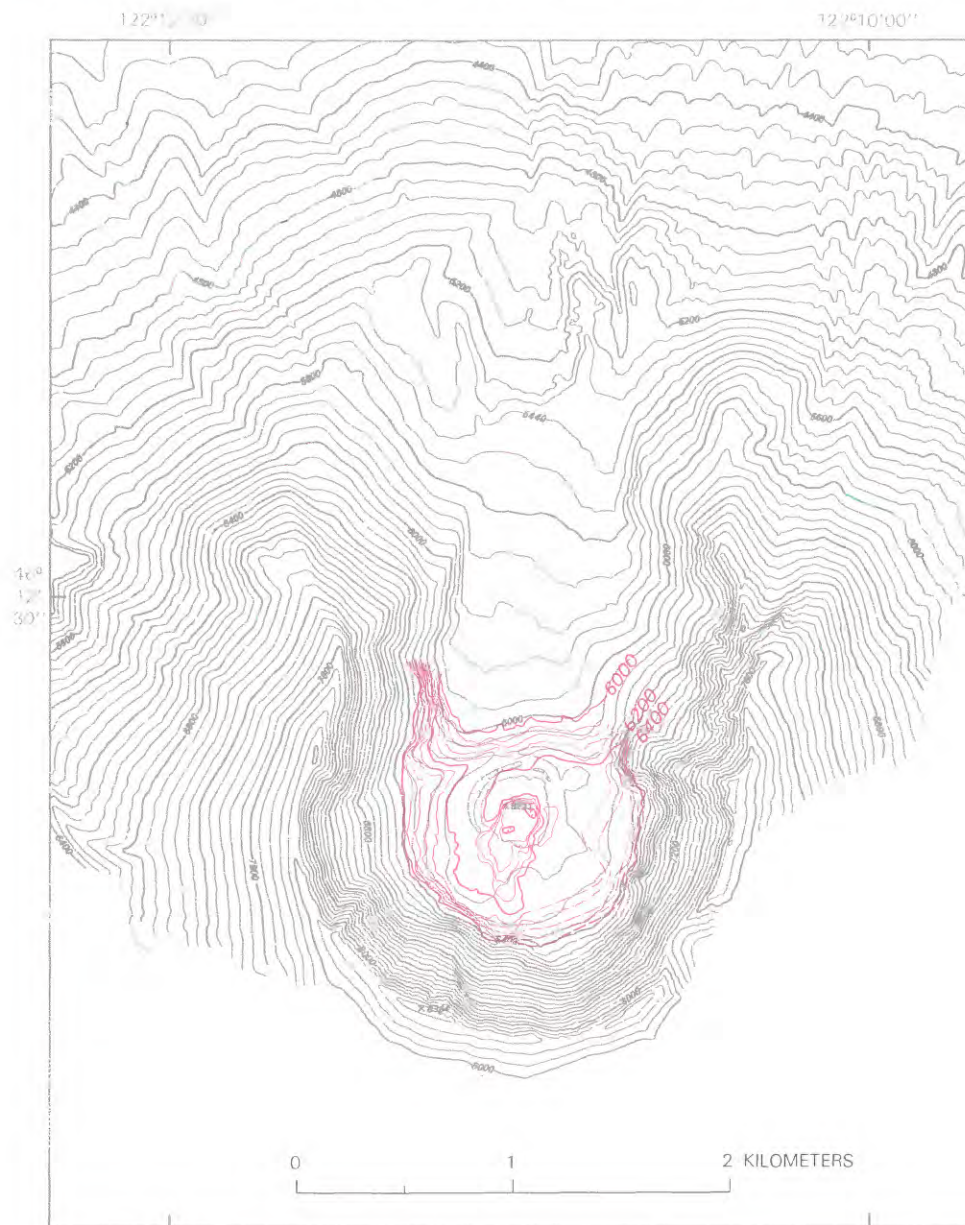


FIGURE 11.—Topographic maps of the area around the vent of Mount St. Helens. Topography in gray prepared from photographs (USGS) taken on July 1, 1980, before the July 22, 1980 eruptions; topography in red prepared from photographs (USGS) taken on July 31, 1980, after the July 22, 1980 eruptions. On the July 31 photographs, part of the crater floor is obscured by volcanic fumes; hence, contours in the obscured area (shown as red dashed lines) could only be located approximately. Map prepared by Diana E. Fair. Contour intervals 80 ft (gray) and 40 ft (red); 1 ft=0.3048 m.

models predict the combinations of vent radius and gas content that will cause a jet of erupted gases and pyroclasts to either rise convectively or undergo gravitational collapse. Column collapse occurs when the condition for convective rise is not met. This condition is that the jet must have, upon deceleration to a minimum upward velocity by drag forces, a density less than that of the ambient atmosphere. Column collapse results in the formation of pyroclastic density flows. The collapse

models assume steady-state conditions, a great depth of magma fragmentation, and an exit pressure of 1 bar. Initially, the eruptions of July 22 and August 7 did not meet the steady-state requirement, were probably derived from shallow depths, and probably had an exit pressure exceeding that of the atmosphere. Thus the models are initially inappropriate for those eruptions. However, the same principles of vent radius and gas content should determine whether collapse or convec-



FIGURE 12.—Mount St. Helens as viewed from Coldwater Peak (about 11 km north of vent) on August 7, 1980, sequence (12A–L) showing the early part of the first eruptive pulse: *A*, 1626:12; *B*, 1626:47; *C*, 1627:55; *D*, 1628:44; *E*, 1629:17; *F*, 1629:27; *G*, 1630:02; *H*, 1630:18; *I*, 1630:33; *J*, 1630:53; *K*, 1631:22; *L*, 1632:15 PDT.



FIGURE 12.—Continued





FIGURE 12.—Continued



FIGURE 12.—Continued





FIGURE 12.—Continued



FIGURE 12.—Continued

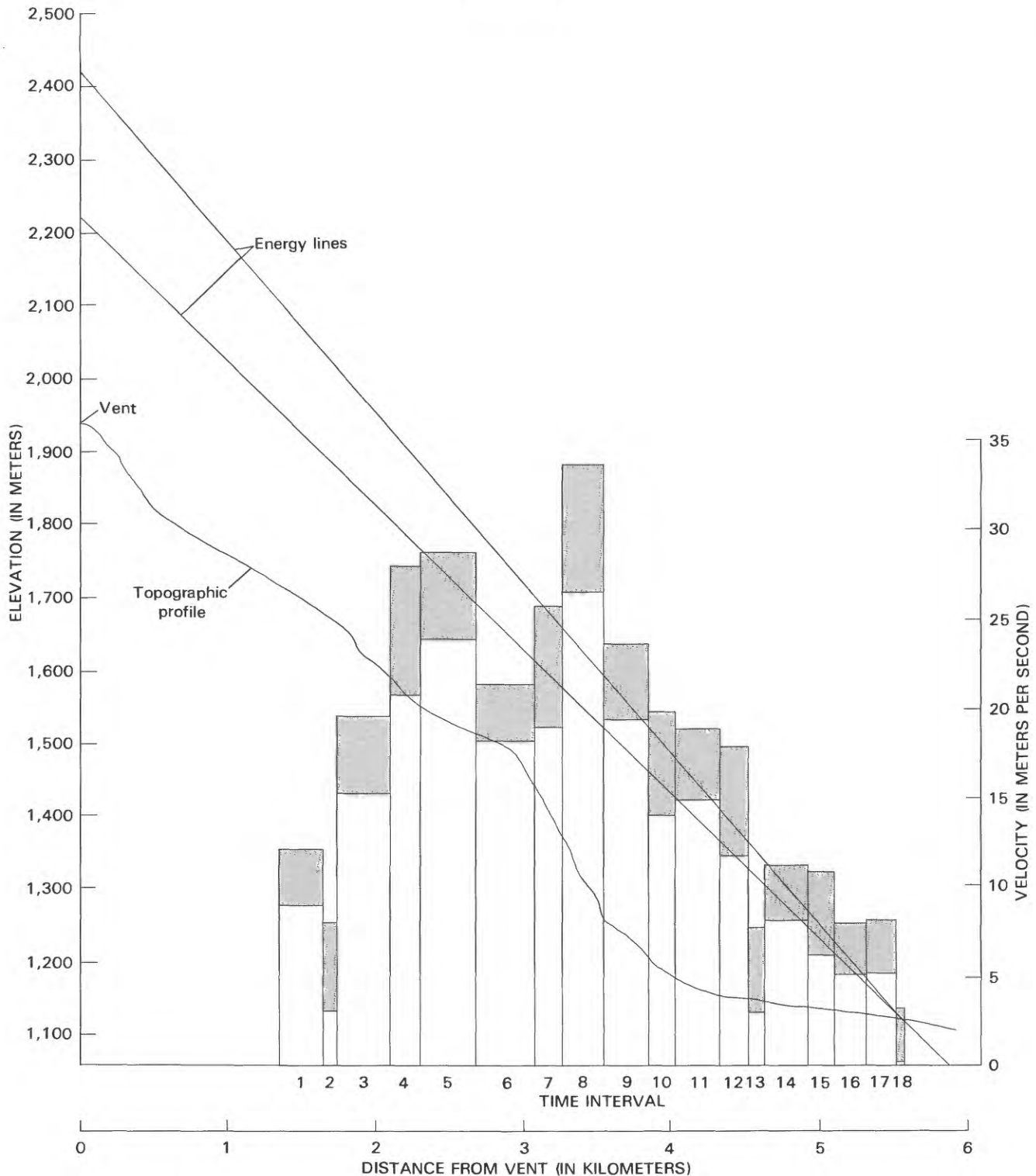


FIGURE 13.—Velocity of the flow front as a function of distance from the vent center for the flow observed on August 7, 1980. Each bar shows a mean velocity for a time interval determined from two sequential, timed photographs. The horizontal distance traversed during a time interval is shown by the bar width, and the terrain traversed during an interval is that portion of the topographic profile delimited by the bar or its extension. Shaded areas at the tops of bars are estimated velocity uncertainties. The two straight diagonal lines are “energy lines” (Hsu, 1975). An energy line is constructed by drawing a line between the terminus of a flow and the top of the pyroclastic fountain that produced the flow. The two energy lines shown correspond to two estimates of the fountain height that probably bracket the range of reasonable fountain-height estimates. According to the energy-line concept, the flow will accelerate if the slope of the topography is greater than that of the energy line, and the flow will come to rest where the energy line intersects the topographic surface. Topographic profile has fivefold vertical exaggeration.



FIGURE 14.—Mount St. Helens as viewed from the north on August 15, 1980. Dashed line shows path followed by the front of the western pyroclastic density flow of August 7. Braces show segments of flow path from which major ash-cloud protuberances emanated.

tion occurs in shallow, high-pressure explosions if the vent-radius variable is redefined as an “effective vent radius” (R. S. J. Sparks, written commun., 1982). This effective vent radius is the radius achieved by the ejected gas/solid mixture upon expansion to a pressure of 1 bar.

The pyroclastic fountains could be considered as eruption jets whose effective vent radii and gas contents were such that convective rise was not possible. However, after the initial collapse, conditions must have changed because convective rise began to occur. According to Wilson and others (1980), a shift from column collapse to convective rise implies that either the vent radius (in this case, effective vent radius) decreased or that the gas content increased. Either or perhaps both changes may have occurred during the eruptions of July 22 and August 7.

The observed change from column collapse to convective rise may have been due to a decrease in the vent radius. This may seem odd because the physical vent radius is likely to widen as an eruption proceeds. However, it is also likely that the explosion depth would increase with time, and so the large effective vent radius of the early, shallow explosions would be succeeded by

the small physical vent radius of the later, deeper explosions. In effect, the radius would decrease with time.

It is also possible that the observed behavior was due to an increase in gas content. At least two explanations for such an increase are possible.

1. The upper part of the magma column could have become depleted in gas between eruptions; thus, less gas would be available to drive the early part of the eruption than the later part. This possibility is consistent with the observation of low-level gas-streaming activity during the repose intervals between eruptions.

2. An initial, unusually high proportion of solids could result from “vent clearing” as fragmental material filling the upper part of the vent was suddenly expelled at the outset of an eruptive pulse. This alternative is supported by the appearance of spearhead projections over the vent immediately prior to the formation of pyroclastic fountains during the third eruptive pulse of July 22. The spearhead projections are clearly due to pressurized gases escaping through pyroclasts. This suggests that the conduit above the magma body may have been choked with pyroclasts at the beginning of the eruption.

The shift from column collapse to convective rise was



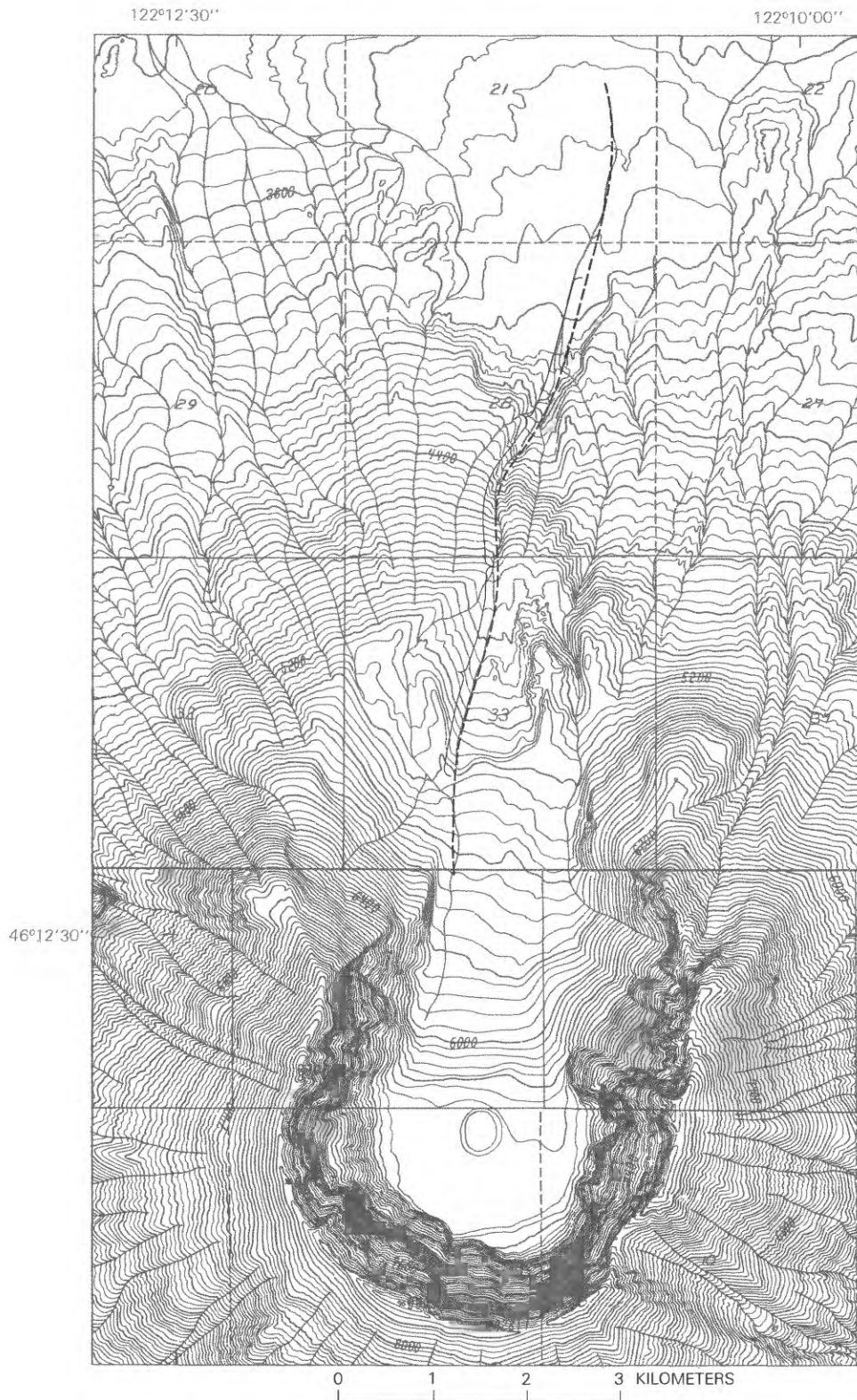


FIGURE 15.—Topographic map of the area around the crater and north flank of Mount St. Helens, prepared from photographs (USGS) taken on September 6, 1980. Dashed line shows path followed by the front of the western pyroclastic density flow of August 7. Braces show segments of flow path from which major ash-cloud protuberances emanated. Contours in feet; 1 ft = 0.3048 m.

probably not due to any single cause. Rather, the three possibilities mentioned above—decrease in vent radius, and increase in gas content from upper magma gas depletion and from vent clearing—probably were all operative to some extent.

#### SPECULATIONS CONCERNING A RELIEF-VALVE MECHANISM

If the conduit above the magma body is choked with pyroclastic debris at the beginning of an eruption, that debris may act as a relief valve. Fluidization experiments show that as gas flows upward through a bed of poorly sorted particles, the system will change behavior as the flow rate is increased (C. J. N. Wilson, 1980). At low flow rates the particles remain stationary. However, as the flow is increased, a rate will eventually be reached at which the drag force of the gas will be sufficient to support the buoyant weight of the smallest particles, and the bed will become partially fluidized. Additional increases will cause the bed to expand until the condition of maximum bed expansion is reached. Until this point, an increase in the flow rate is accompanied by an increase in the vertical pressure difference across the bed. However, as the flow rate is increased beyond the point of maximum bed expansion, the gas begins to segregate into bubbles and channels, and the pressure drop across the bed decreases sharply.

It is possible that an analogous process operates at the outset of eruptions if the conduit above the magma body is filled with pyroclastic debris. Vesiculation of the magma would cause gas to flow through this bed of debris and escape to the atmosphere (fig. 16A). If the rate at which the magma produced gas exceeded the rate at which gas escaped, the pressure difference across the bed would increase, as would the flow rate. Eventually the flow rate would increase to a value that would cause formation of gas bubbles and channels through the bed of pyroclasts (fig. 16B). This would cause a rapid decrease in the pressure difference across the bed, and the magma would experience a sudden decompression, as the ability of the debris bed to contain the accumulated gases became drastically reduced. The upper

part of the decompressed magma body would begin to fragment and suddenly liberate more gas, which would further increase the flow rate. When the rate of gas flow became great enough, it would begin to expel the vent-filling bed of pyroclasts (fig. 16C). If this ejected mass of gases and pyroclasts had a relatively high particle concentration, and did not meet the requirements for convective rise, it would form a pyroclastic fountain. The fountaining gas/solid suspension would generate a pyroclastic density flow. After the vent was cleared, the relatively low particle concentration of the continuing eruption jet could meet the requirements for convective rise, and a vertical-eruption column would develop (fig. 16D).

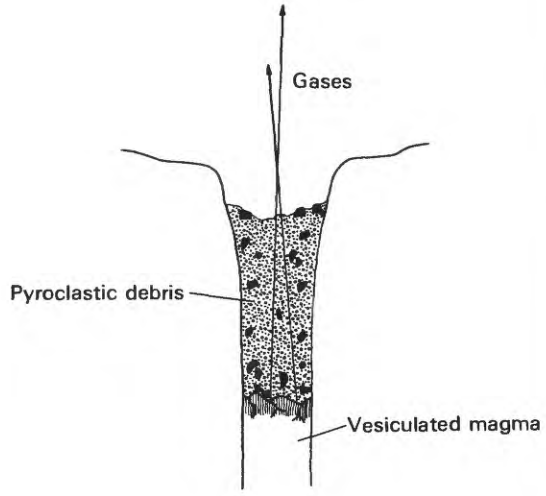
The eruption would be modulated into a series of pulses if the gas-loss rate during eruptions exceeded the rate at which gas is produced by vesiculation. As the eruption tapped progressively deeper levels of the magma body, progressively less vesicular magma would be available to drive the eruption. The gas content of the eruption jet would therefore begin to decrease. Eventually the gas content would decline to a value that would be inadequate to eject the largest fragments from the vent. This process would continue, with progressively smaller fragments remaining in the vent, until the vent again became choked with pyroclasts (fig. 16A). In effect, the pyroclastic debris has acted as a relief valve. The eruption/repose sequence would continue until gas-production rates had become inadequate to open the relief valve, either because the depth of the bed of pyroclasts had become too great, the volatile content of the magma had become too low, or the magma had been expended.

The eruptions of Mount St. Helens provide several lines of evidence that support the relief-valve hypothesis.

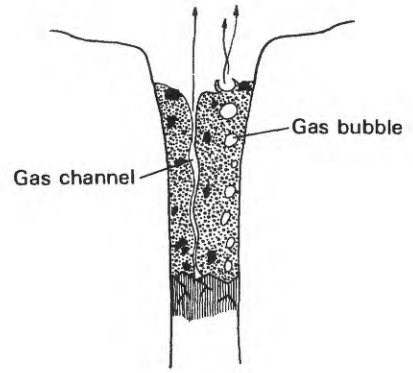
1. The relief-valve mechanism would modulate an eruption into a series of pulses separated by periods of relative quiescence. Multiple eruptive pulses occurred at Mount St. Helens on July 22, August 7, and October 16–18, 1980.

2. Mild gas-streaming activity would be expected during periods of quiescence between eruptive pulses. This was observed on July 22.

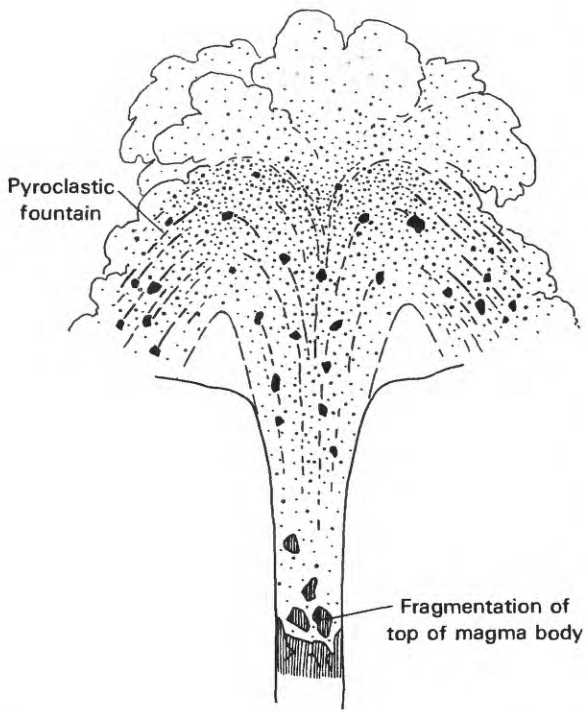
FIGURE 16.—Hypothetical relief-valve mechanism: *A*, Vent above magma body is choked with pyroclastic debris. Vesiculation in the upper part of the magma body releases gases, which flow up through debris. The vertical pressure difference across the debris, and the gas flow rate, increase as vesiculation proceeds. Debris remains stationary and volcano is in repose. *B*, Continuing vesiculation has increased flow rate to a value that causes formation of gas bubbles and channels through debris. Pressure difference across the debris bed decreases sharply. *C*, Decompression of the magma triggers fragmentation of the vesiculated magma. Gases liberated by the fragmentation further increase the flow rate. This causes vent-filling debris to be expelled as a gas/solid mixture (pyroclastic fountain) whose density is greater than air. A pyroclastic density flow (not shown) is formed as an eruption begins. *D*, As the vent is cleared of the debris, the density of the eruption jet decreases until the condition for convective rise is met. As the eruption taps progressively less vesicular magma, the gas content decreases until debris is not expelled as quickly as it is produced. This leads to the reestablishment of the condition shown in step *A*.



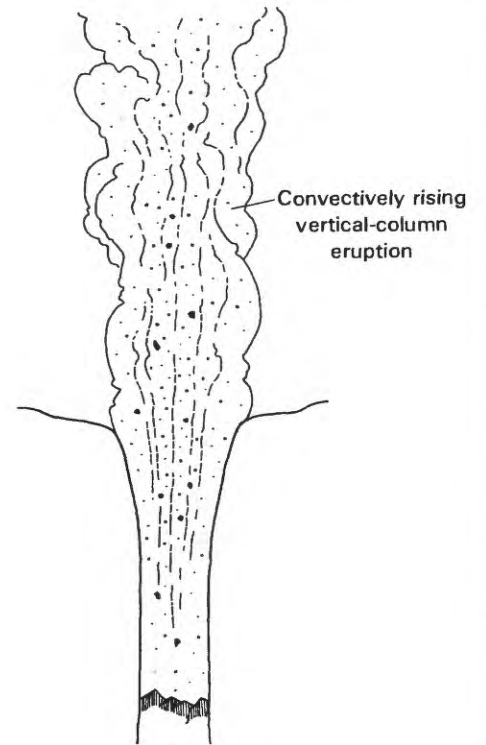
A



B



C



D



3. Partial fluidization of the vent-filling debris would immediately precede an eruptive pulse. This was observed just prior to the third eruptive pulse of July 22.

4. Pyroclastic density flows would be generated before a convectively driven vertical-eruption column appeared. This occurred at least twice on July 22, and at least once on August 7.

5. If a pyroclastic density flow is formed by the relief-valve mechanism, the volume of the resultant flow deposit should approximate the volume of the vent-filling debris from which it was derived. This relationship, along with the vent diameter, makes it possible to calculate the approximate depth of the hypothetical debris bed that forms the relief valve. Small depth values would favor the relief-valve mechanism, whereas large depth values would favor some other mechanism. The volumes of pyroclastic flows generated by the second and third eruptive pulses of July 22 were each about 0.003 km<sup>3</sup> (Rowley and others, 1981, p. 497). A reasonable vent-radius estimate is about 50 m. Thus, a bed depth of only about 400 m would be necessary to produce the observed flow-deposit volume.

The relief-valve mechanism could not have operated at the outset of the first eruptive pulse of July 22 because the vent was blocked by a dome. Observations indicate that a density flow formed early during this pulse. However, this flow was quite small as compared to those produced by the second and third eruptive pulses of July 22 and the first pulse of August 7, when the vent was not blocked by a dome. One interpretation is that the difference in the size of the flows is due to the eruptive mechanism. That is, the small density flow was formed from fragmental debris produced by the explosive disruption of the dome, whereas the succeeding larger flows were products of the relief-valve mechanism. The relief valve would presumably eject a larger volume of fragmental material than would be produced by a shallow dome explosion.

The relief-valve mechanism is apt to operate only if the maximum vertical pressure difference that can develop across the debris column is a significant fraction of the pressure that can develop at the upper surface of the magma body. Apparently, no method currently exists to calculate the maximum pressure drop that can be maintained across a bed of poorly sorted pyroclasts. However, fluidization experiments on ignimbrite fines (C. J. N. Wilson, 1980) suggest that a value of about 0.1 bar per meter of bed depth is reasonable. Thus, rather thin beds of vent debris are capable of containing substantial gas pressures. For example, thicknesses of a few hundreds of meters would contain pressure drops of a few tens of bars. Such values are of the same order as those predicted (Wilson and others, 1980)

for the upper surface of a rhyolitic magma with a low volatile content (about 1 percent).

The closest antecedent to the proposed relief-valve mechanism is that suggested by Eichelberger and Westrich (1981). They suggested pulsating eruptive behavior to explain an upward increase in the proportion of dense fragments in pyroclastic deposits of rhyolitic magma of low volatile content. Further, they proposed that the inferred pulsating behavior was a result of eruption rates that exceeded vesiculation rates.

#### FEATURES ASSOCIATED WITH THE FRONT OF THE PYROCLASTIC DENSITY FLOW FORMED BY THE THIRD ERUPTIVE PULSE OF JULY 22, 1980

Some of the most intriguing phenomena associated with the pyroclastic density flows were the light-colored features that appeared ahead of the flow front during the third eruptive pulse of July 22. These features included a diffuse zone immediately ahead of the flow front and a series of discontinuous bands that preceded and merged with the diffuse zone (best displayed on fig. 9E). The mechanism responsible for the bands is not known, but they could have been caused by displacement of air by the advancing flow. Presumably, the wind generated by the displacement eroded and transported loose ash from previously emplaced deposits.

The diffuse zone immediately ahead of the flow front locally exhibited striae or rays normal to the front (fig. 9D). The diffuse zone may be a manifestation of "separated flow." Separated flow has been postulated by Allen (1971a) as one of two possible solutions for the flow field in the host medium ahead of a density flow with an overhanging head. This type of separated flow (fig. 17A) requires that air below the flow-front overhang be pushed ahead of the front. Such separated flows have been aptly termed "rollers" (Allen, 1971b). I suggest that the roller was made visible by the ash caught up in it. The striae or rays that seem to radiate from the front of the pyroclastic flow are envisaged as streams of ash mobilized by the basal part of the roller, whose flow direction parallels that of the front of the pyroclastic density flow. Allen (1971a) concluded that observations of density flows favored an alternative ("mass flow") solution, which involves a lobe-and-cleft head structure (cleft: fig. 17B; lobe: fig. 17C). In this solution, air below the flow-front overhang is channeled into the clefts and overridden by the flow. In the example that I witnessed, the diffuse zone ahead of the flow front, which may have been caused by a roller, appeared even though the flow front exhibited lobe-and-cleft structures. Both solutions apparently operated concurrently.



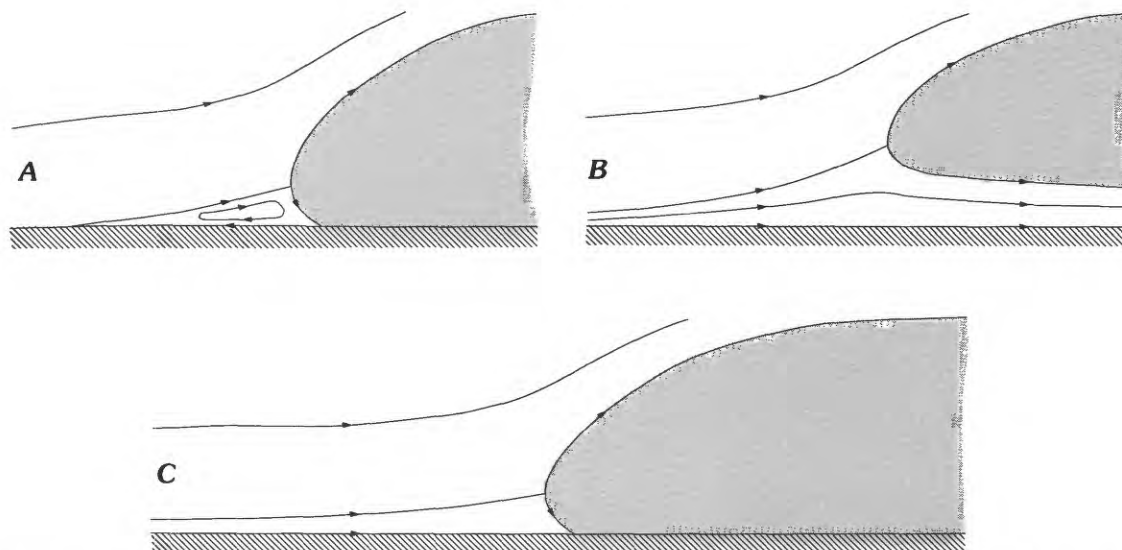


FIGURE 17.—Two alternative solutions for the flow field in the host medium of a density flow. Head of density flow is shaded. The velocity of the host medium is assigned a value equal but opposite to that of the head, so the head is stationary. Streamlines are drawn relative to the stationary head. *A*, Solution involving separated flow. *B*, *C*, Solution for flow on axes of clefts and lobes, respectively. (Modified from Allen, 1971a.)

Whatever processes were actually responsible for the phenomena that preceded the front of the density flow, probably too little debris was mobilized to have produced a recognizable deposit. However, these processes might produce significant deposits if they were associated with large-scale flows.

#### TEMPERATURES OF THE PYROCLASTIC-FLOW DEPOSITS OF JULY 22, 1980

The temperature data obtained from the pyroclastic-flow deposits of July 22 provide some evidence of the heat-transfer processes that operated on the pyroclasts. The most reasonable interpretation is that the debris mixed with and transferred heat to air. The emplacement-temperature inhomogeneities reflect the fact that (1) small particles, because of their greater surface-area/volume ratio, transfer heat more efficiently than do large fragments, and (2) insufficient time had elapsed prior to the measurements for temperature equilibration to occur. The greatest lateral emplacement-temperature gradient within a given deposit was observed near the vent (Banks and Hoblitt, 1981). This suggests that most cooling occurred near the vent, probably as fountaining ejecta mixed with air to form a turbulent suspension of gases and pyroclasts. This may explain why the pyroclastic-flow deposit produced by the third eruptive pulse was, in general, emplaced at a higher temperature than that of the

second pulse. The second pulse produced a somewhat higher fountain than the third (table 1), and thus had a greater opportunity to mix with air. The pyroclastic-flow deposit of the second pulse also appeared to be finer grained than that of the third. Thus, the debris of the second pulse had a greater aggregate heat-transfer efficiency than that of the third. The importance of air cooling in pyroclastic flows was first suggested by Smith (1960) as an explanation for the discrepancies between the welding patterns observed in ash flows and those expected from theory. The emplacement-temperature predictions of Sparks and others (1978) are, at least qualitatively, in accord with the temperature data and interpretations presented here.

#### A POSSIBLE GENETIC RELATIONSHIP BETWEEN PYROCLASTIC FLOWS AND PYROCLASTIC SURGES DURING THE ERUPTION OF AUGUST 7, 1980

The sequence of timed photographs obtained on August 7 yielded an almost complete velocity history for one flow.<sup>5</sup> This history apparently is more detailed than any velocity record of a similar event. In general,

<sup>5</sup>In this discussion it is important to remember that the term "flow" without a modifier is used as a synonym for "density flow"; that is, as a nonspecific term for pyroclastic flow or pyroclastic surge.

the flow-front velocity is directly related to topographic slope (fig. 13). Two cycles of acceleration and deceleration occurred over the two steep parts of the flow path; each acceleration and deceleration corresponds to an increase and decrease, respectively, of the slope. These velocity data can be compared to the predictions of the energy-line concept of Hsu (1975), which has been summarized by Sheridan (1980, p. 400) as follows:

"A density flow initiated at some elevation will move as potential energy is converted to kinetic energy minus friction. The energy line is the slope along which the frictional loss is balanced by conversion of potential to kinetic energy. \*\*\*\*The slope of the energy line is calculated as the arc tan of the loss in height ( $H$ ) divided by run-out distance ( $L$ )."

A flow will accelerate (decelerate) as it travels over terrain whose slope is greater than (less than) that of the energy line; it will come to rest where the topographic surface intersects the energy line.

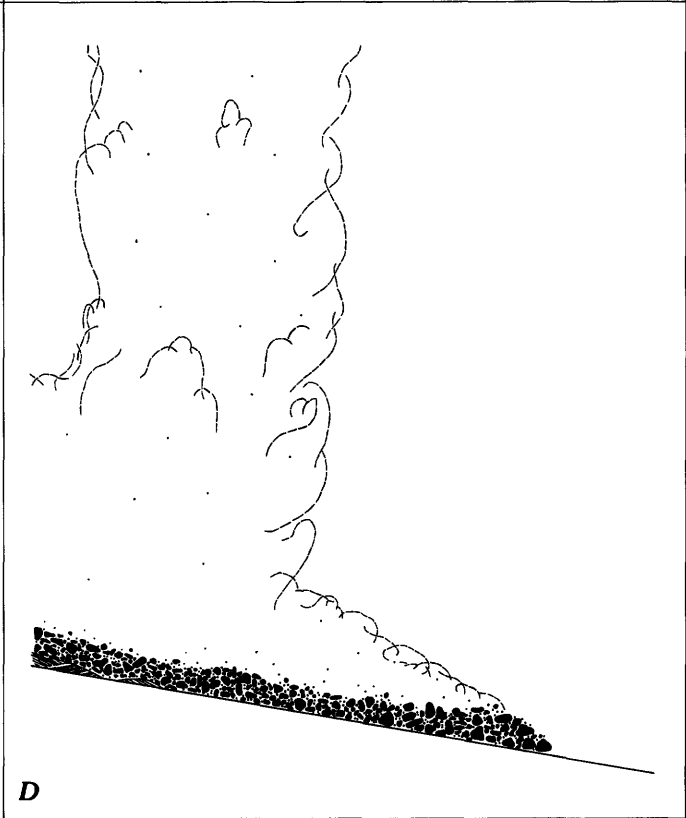
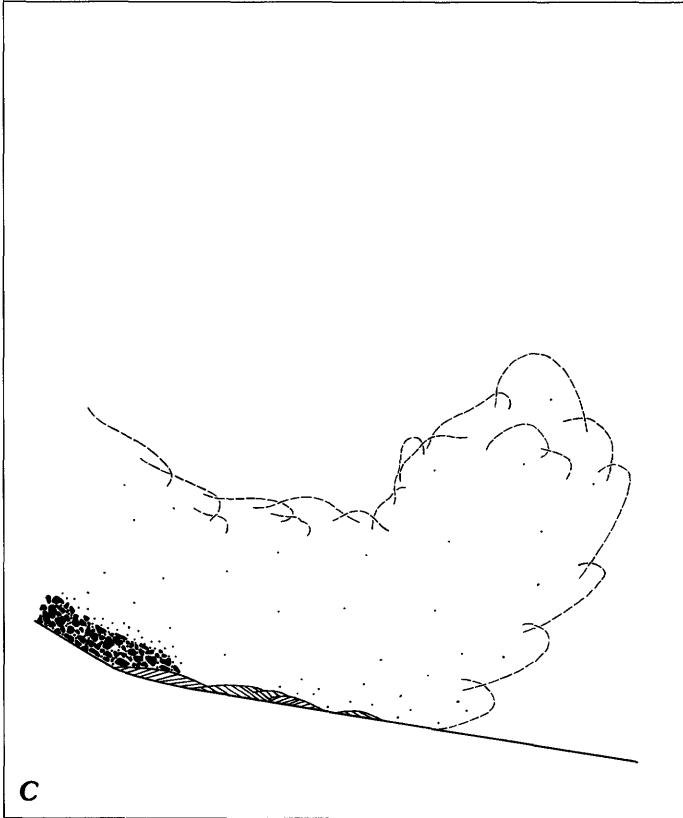
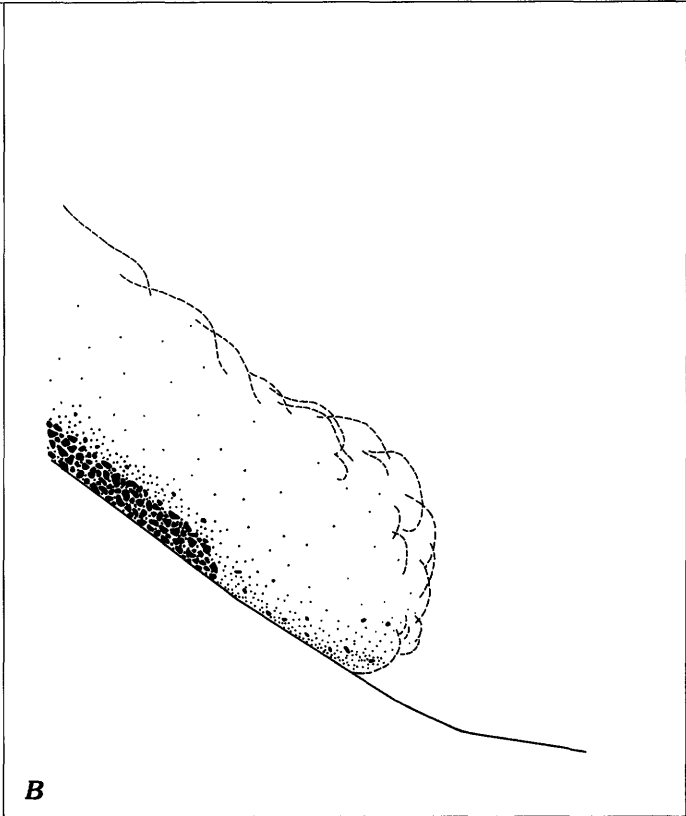
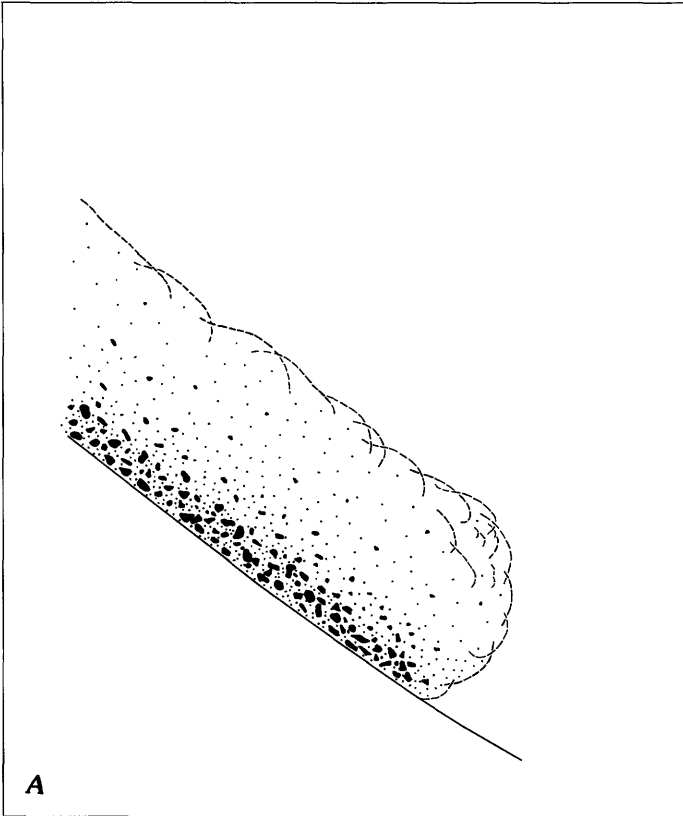
For the flow of August 7, the selection of a value for  $H$  is somewhat arbitrary because of an uncertainty in the height of the pyroclastic fountain above the vent. I have made two fountain-height estimates that probably bracket the range of reasonable values (table 1). The energy lines that correspond to the two estimates have been plotted in figure 13. Overall, the acceleration predictions derived from comparison of the energy line and topographic slopes are fairly accurate, particularly from the energy line based on the lower estimate of fountain height. However, the low value of time interval 13 on the velocity profile is anomalous. Interval 13 marks the end of the second acceleration/deceleration cycle and a change in flow behavior. The deceleration is not surprising, but the subsequent acceleration is unexpected because it is not related to an increase in slope. A possible explanation for the velocity change lies in the concomitant change in the appearance of the flow front. The voluminous, billowing, colloform clouds that marked the flow front ceased to advance and began to rise. Concurrently, the front became thin, wedge shaped, and digitate, and was followed by only small ash clouds. I suggest that these changes in velocity and appearance occurred when a pyroclastic surge derived from and preceding the pyroclastic flow was overtaken by the pyroclastic flow.

As a pyroclastic flow travels down a steep slope, its gas content can increase. This could partly be due to an

increase in the trituration rate of pumice, and a consequent increase in the release rate of juvenile gases. Another important source is air incorporated by the moving mass. During the flow of August 7, air was overridden and incorporated as the flow plunged off cliffs and splashed over obstacles. Analyses of gases from rootless fumaroles in the pyroclastic-flow deposit of June 12, 1980, showed air to be the dominant component (Casadevall and Greenland, 1981, p. 222). Air probably was also an important component of the flow of August 7 because that flow followed the same path as the flow of June 12. Whatever the mechanism, an increase in the gas/solid ratio almost certainly occurred as the August 7 flow descended the steeper portions of the flow path. It is inferred that the resultant expansion would produce an inflated, turbulent suspension of hot gases and pyroclasts, and that the pyroclasts would settle differentially according to their size and density. A high-particle-concentration, coarse-grained phase moving along the ground surface would grade vertically into a fine-grained suspension of lower concentration. The uppermost part of this hot suspension, whose net density would be less than that of the ambient air, would rise convectively. The remainder of the low-particle-concentration part of the flow would be less subject to energy losses through internal friction than the basal flow, and so would accelerate away from the basal flow. Thus, the hot, low-concentration suspension—a pyroclastic surge—would separate from and "surge" ahead of the high-concentration phase—a pyroclastic flow. The hot surge cloud would lose mass through deposition until it became less dense than the ambient air. At this point it would rise, decelerate, and be overtaken by its parent pyroclastic flow.

This hypothetical sequence (fig. 18)—inflation, segregation, separation, and differential acceleration—may have been repeated three times in the flow of August 7. The first sequence was initiated by the pyroclastic fountain as it generated a turbulent, inflated mixture of air and ejecta around the vent. This segregated into both a pyroclastic flow and a pyroclastic surge. The surge initially accelerated and moved in front of the pyroclastic flow. Then, on the gently sloping floor of the amphitheater, the surge decelerated and was overtaken by the pyroclastic flow. Unfortunately, the detailed velocity data shown on figure 13 begin (time interval 1) at the end of this sequence, as the pyroclastic flow overtook

FIGURE 18.—Mechanism that may have operated during the flow observed on August 7, 1980. *A*, Highly inflated suspension generated by collapse of pyroclastic fountain or by passage of pyroclastic flow over steep, irregular terrain. *B*, Segregation of the suspension into high- and low-concentration phases. *C*, Low-concentration phase (pyroclastic surge) that has separated from high-concentration phase (pyroclastic flow) deposits surge beds until it becomes less dense than air, rises, and decelerates. *D*, Rising remnant of pyroclastic-surge cloud is overtaken by pyroclastic flow.



the stagnating surge. The details of the early velocity history could not be determined because of poor viewing conditions. However, the mean velocity from the beginning of fountain formation to the time that the flow front first became clearly visible is 30 m/s. The velocity was low when the flow front became clearly visible, so the velocity shortly after fountain collapse must have been greater than 30 m/s, which is about the highest velocity determined from the clearly visible flow front (fig. 13). Thus the highest velocity was probably achieved soon after fountain collapse; this was followed by a deceleration and a subsequent acceleration of the flow front.

A second surge was probably initiated as the pyroclastic flow crossed an abrupt break in slope at the 1,650-m level. A third and final pyroclastic surge was initiated as the pyroclastic flow descended the stair steps—the steepest, most irregular part of the flow path. In contrast to the first surge, which was derived directly from the pyroclastic fountain, the second and third surges were derived from the pyroclastic flow. The acceleration/deceleration cycles of the second and third surges are shown on figure 13.

The hypothetical inflation, segregation, separation, and differential acceleration sequence is consistent with the behavior of the ash-cloud protuberances that were described previously in this report. The two major protuberances originated from the parts of the path that were traversed by the postulated surge clouds. The parts of the path in which only small ash clouds were produced were traversed solely by the pyroclastic flow. The ash cloud produced by the collapse of the pyroclastic fountain could also be considered as a protuberance; this merged upward into the vertical-eruption column that developed after the pyroclastic fountain.

Little stratigraphic evidence is available to test the proposed pyroclastic-flow/pyroclastic-surge relationship. The flow of August 7 produced both pyroclastic-surge and pyroclastic-flow deposits; the distribution of the pyroclastic-flow deposits is known in detail, but little is known of the distribution of the pyroclastic-surge deposits. I identified surge deposits from the eruption of August 7 at the apex of the pumice plain. The presence of pyroclastic-surge deposits at this location is consistent with my interpretation of the velocity data.

The possible genetic pyroclastic-flow/pyroclastic-surge relationship during the eruption of August 7 is consistent with the following models and observational data.

1. Similar segregation and separation models have previously been described by Fisher, 1976, 1979, p. 311-313; Sparks and others, 1978, p. 1735; Wohletz and Sheridan, 1979; Fisher and others, 1980, p. 475; and Fisher and Heiken, 1982, p. 365-367.

2. Accounts of explosive stratovolcanic eruptions indicate that flow separation is a common phenomenon (for example, Anderson and Flett, 1903, p. 511; MacDonald and Alcaez, 1956, p. 174; Moore and Melson, 1969, p. 616-617).

3. On the basis of stratigraphic relationships, Sparks and others (1973) suggested that a pyroclastic flow is often accompanied and preceded by a pyroclastic surge.

4. A momentary pause in the rate of flow advance, which follows an initial rapid advance, has been observed at the outset of other eruptions (Perret, 1937, p. 91-92). Such a pause was probably caused by the deceleration of a pyroclastic surge, which was subsequently overtaken by a cogenetic pyroclastic flow. Both the pyroclastic flow and pyroclastic surge are probably generated simultaneously by a pyroclastic fountain.

The ingestion of air and resultant dilution of a flow probably occurs wherever a flow passes over surfaces whose relief is a significant fraction of the flow thickness. This may occur on the flanks of the source volcano or on the surrounding terrain. A pyroclastic flow may thus spawn one or more pyroclastic surges at locations remote from the volcano. This dilution probably occurs in pyroclastic surges as well as pyroclastic flows. The ingestion of air by a pyroclastic surge would increase the time that particles would be held in suspension and, thus, extend the lifetime and length of the pyroclastic surge.

## REFERENCES CITED

- Allen, J. R. L., 1971a, Mixing at turbidity current heads, and its geological implications: *Journal of Sedimentary Petrology*, v. 41, no. 1, p. 97-113.
- , 1971b, Transverse erosional marks of mud and rock—Their physical basis and geological significance: *Sedimentary Geology*, v. 5, p. 167-385.
- Anderson, Tempest, and Flett, J. S., 1903, Report on the eruption of the Soufrière in St. Vincent in 1902 and on a visit to Montagne Pelée in Martinique: *Philosophical Transactions of the Royal Society of London*, ser. A, v. 200, p. 353-553.
- Banks, N. G., and Hoblitt, R. P., 1981, Summary of temperature studies of 1980 deposits, in Lipman, P. W., and Mullineaux, D. R., eds., *The 1980 eruptions of Mount St. Helens, Washington*: U.S. Geological Survey Professional Paper 1250, p. 295-313.
- Casadevall, T. J., and Greenland, L. P., 1981, The chemistry of gases emanating from Mount St. Helens, May-September 1980, in Lipman, P. W., and Mullineaux, D. R., eds., *The 1980 eruptions of Mount St. Helens, Washington*: U.S. Geological Survey Professional Paper 1250, p. 221-226.
- Christiansen, R. L., and Peterson, D. W., 1981, Chronology of the 1980 eruptive activity, in Lipman, P. W., and Mullineaux, D. R., eds., *The 1980 eruptions of Mount St. Helens, Washington*: U.S. Geological Survey Professional Paper 1250, p. 17-30.
- Eichelberger, J. C., and Westrich, H. R., 1981, Magmatic volatiles in explosive rhyolitic eruptions: *Geophysical Research Letter*, v. 8, no. 7, p. 757-760.

- Fisher, R. V., 1976, The mobility of hot pyroclastic flows [abs.]: *Geological Society of America Abstracts with Programs*, v. 8, no. 5, p. 586.
- \_\_\_\_\_, 1977, Erosion by volcanic base-surge density currents—U-shaped channels: *Geological Society of America Bulletin*, v. 88, p. 1287-1297.
- \_\_\_\_\_, 1979, Models for pyroclastic surges and pyroclastic flows: *Journal of Volcanology and Geothermal Research*, v. 6, p. 305-318.
- Fisher, R. V., and Heiken, Grant, 1982, Mt. Pelée, Martinique—May 18 and 20, 1902, pyroclastic flows and surges: *Journal of Volcanology and Geothermal Research*, v. 13, p. 339-371.
- Fisher, R. V., Smith, A. L., and Roobol, M. J., 1980, Destruction of St. Pierre, Martinique, by ash-cloud surges, May 8 and 20, 1902: *Geology*, v. 8, p. 472-476.
- Harris, D. M., Roe, Robert, and Rose, W. I., Jr., 1980, Radar observations of the July 22 and Aug. 7, 1980 eruptions of Mount St. Helens: *EOS, American Geophysical Union Transactions*, v. 61, no. 46, p. 1137.
- Harris, D. M., Rose, W. I., Jr., Roe, Robert, and Thompson, M. R., 1981, Radar observations of ash eruptions, in Lipman, P. W., and Mullineaux, D. R., eds., *The 1980 eruptions of Mount St. Helens*, Washington: U.S. Geological Survey Professional Paper 1250, p. 323-333.
- Hsu, K. J., 1975, Catastrophic debris streams (sturzstroms) generated by rockfalls: *Geological Society America Bulletin*, v. 86, p. 129-140.
- Kuntz, M. A., Rowley, P. D., MacLeod, N. S., Reynolds, R. L., Mcbroome, L. A., Kaplan, A. M., and Lidke, D. J., 1981, Petrography and particle-size distribution of pyroclastic flow, ash-cloud, and surge deposits, in Lipman, P. W., and Mullineaux, D. R., eds., *The 1980 eruptions of Mount St. Helens*, Washington: U.S. Geological Survey Professional Paper 1250, p. 525-539.
- MacDonald, G. A., and Alcaez, Arturo, 1956, Nuées ardentes of the 1948-1953 eruption of Hibok-Hibok: *Bulletin Volcanologique*, v. 18, p. 169-178.
- Malone, S. D., Endo, E. T., Weaver, C. S., and Ramey, J. W., 1981, Seismic monitoring for eruption prediction, in Lipman, P. W., and Mullineaux, D. R., eds., *The 1980 eruptions of Mount St. Helens*, Washington: U.S. Geological Survey Professional Paper 1250, p. 803-813.
- Moore, J. G., Lipman, P. W., Swanson, D. A., and Alpha, T. R., 1981, Growth of lava domes in the crater, June 1980-January 1981, in Lipman, P. W., and Mullineaux, D. R., eds., *The 1980 eruptions of Mount St. Helens*, Washington: U.S. Geological Survey Professional Paper 1250, p. 541-556.
- Moore, J. G., and Melson, W. G., 1969, Nuées ardentes of the 1968 eruption of Mayon volcano, Philippines: *Bulletin Volcanologique*, v. 33, p. 600-620.
- Nairn, I. A., and Self, Stephen, 1978, Explosive eruptions and pyroclastic avalanches from Ngauruhoe in February 1975: *Journal of Volcanology and Geothermal Research*, v. 3, p. 39-60.
- Perret, F. A., 1937, The eruption of Mt. Pelee 1929-1932: *Carnegie Institution of Washington Pub. no. 458*, 126 p.
- Rowley, P. D., Kuntz, M. A., and MacLeod, N. S., 1981, Pyroclastic flow deposits, in Lipman, P. W., and Mullineaux, D. R., eds., *The 1980 eruptions of Mount St. Helens*, Washington: U.S. Geological Survey Professional Paper 1250, p. 489-512.
- Sheridan, M. F., 1979, Emplacement of pyroclastic flows—A review: *Geological Society of America Special Paper 180*, p. 125-136.
- \_\_\_\_\_, 1980, Pyroclastic block flow from the September, 1976, eruption of La Soufriere volcano, Guadeloupe: *Bulletin Volcanologique*, v. 43-2, p. 397-402.
- Simpson, J. E., 1969, A comparison between laboratory and atmospheric density currents: *Quarterly Journal of the Royal Meteorological Society*, v. 95, p. 758-765.
- Smith, R. L., 1960, Ash-flows: *Geological Society of America Bulletin*, v. 71, p. 795-842.
- Sparks, R. S. J., Self, Stephen, and Walker, G. P. L., 1973, Products of ignimbrite eruptions: *Geology*, v. 1, no. 3, p. 115-118.
- Sparks, R. S. J., and Wilson, Lionel, 1976, A model for the formation of ignimbrite by gravitational column collapse: *Geological Society of London Journal*, v. 132, p. 441-451.
- Sparks, R. S. J., Wilson, Lionel, and Hulme, G., 1978, Theoretical modeling of the generation, movement, and emplacement of pyroclastic flows by column collapse: *Journal of Geophysical Research*, v. 83, no. B4, p. 1727-1739.
- Taylor, G. A., 1958, The 1951 eruption of Mount Lamington, Papua: *Australia Bureau of Mineral Resources, Geology, and Geophysics Bulletin 38*, 117 p.
- Volk, William, 1958, *Applied statistics for engineers*: New York, McGraw-Hill, 354 p.
- Wilson, C. J. N., 1980, The role of fluidization in the emplacement of pyroclastic flows—An experimental approach: *Journal of Volcanology and Geothermal Research*, v. 8, p. 231-249.
- Wilson, Lionel, and Head, J. W., 1981, Morphology and rheology of pyroclastic flows and their deposits, and guidelines for future observations, in Lipman, P. W., and Mullineaux, D. R., eds., *The 1980 eruptions of Mount St. Helens*, Washington: U.S. Geological Survey Professional Paper 1250, p. 513-524.
- Wilson, Lionel, Sparks, R. S. J., and Walker, G. P. L., 1980, Explosive volcanic eruptions - IV. The control of magma properties and conduit geometry on eruption column behavior: *Geophysical Journal of the Royal Astronomical Society*, v. 63, p. 117-148.
- Wohletz, K. H., and Sheridan, M. F., 1979, A model for pyroclastic surge: *Geological Society of America Special Paper 180*, p. 177-194.





---

---

## APPENDIX

---

---

### APPENDIX.—DETERMINATION OF THE VELOCITY OF THE PYROCLASTIC DENSITY FLOW

Because the time intervals between photographs are known to within  $\pm 0.5$  s, flow-velocity determination was reduced to the problem of establishing the distance covered by the flow front between successive exposures. This is not a trivial problem. Except for a few photographs, insufficient landmarks are available to accurately locate the position of the front on a topographic map.

The photographs are 35-mm slides that were taken with a hand-held, clock-equipped camera. The camera was approximately horizontal and the aiming point was approximately the same for all photographs. The first slide was projected, and the flow front and salient reference features (such as the silhouette of the mountain) were traced onto a sheet of paper. On projections of succeeding photographs, the paper was moved so that

the traced reference features were superimposed, then the new position of the flow front was traced (as in fig. 19).

The leading point of the flow front on each tracing was identified; together these points constituted the flow path. By inspection, this path was located on the available topographic map that best represented the topography at the time of eruption (fig. 15; shown diagrammatically on fig. 20).

It was then necessary to prepare a topographic profile that, ideally, would include the flow path and the point from which the photographs were taken (Coldwater Peak). Because these points do not all lie on a single vertical plane, a vertical plane was chosen that included the Coldwater Peak camera station and that passed through an "average" flow path chosen by inspection (fig. 20). The topographic contours intersected by the flow path were orthographically projected onto this plane, then the profile (fig. 21) was constructed.

Lines were then drawn from each contour point on the profile to the camera site. These lines represent the

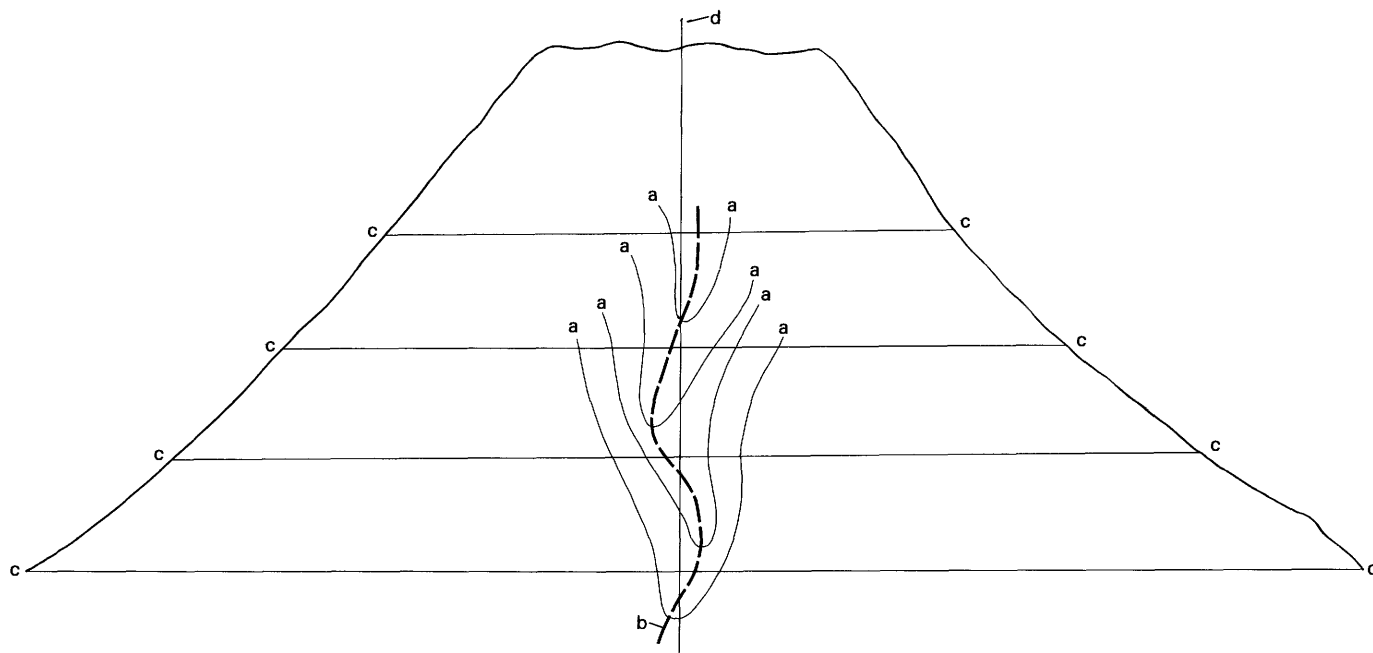


FIGURE 19.—Procedure used to extract flow-front positions from photographs: a, tracings of flow margins as they appeared on successive photographs; b, flow path determined by drawing a line through successive flow-front positions; c, topographic contours as viewed from the camera station; and d, vertical-projection plans as viewed from the camera station.

paths of light rays to the camera. The next step was to draw a vertical line to obtain its intersection points with the rays. Any vertical line will do. Parallel lines with the same spacings as the intersection points were placed on a transparent overlay. These lines show the spacing between specific topographic contours traversed by the flow front as seen from the camera station. The overlay was then optically projected onto the composite tracing of the flow fronts (fig. 19), and the scale was optically adjusted until two or more flow-front positions of known altitude matched the altitudes given by the overlay points. The altitudes of all other flow-front tracings were then read from the overlay. These altitudes could now be found on the flow path (fig. 20), and the distances between successive flow-front positions could be determined.

The accuracy of the results was not significantly affected by the selection of flow path or projection plane because the altitudes of interest were similar to the altitude of the Coldwater Peak camera site. Thus, as seen from the camera station, topographic contour lines traversed by the flow were essentially straight lines. Varying the flow path or the position of the vertical-projection plane would not significantly change the altitude estimates. The uncertainty in the distance between successive flow-front positions is estimated to be  $\pm 50$  m (based on the uncertainty in locating flow-front positions on the few photographs with adequate landmarks). The resulting uncertainty in the velocity was calculated according to the procedure of Volk (1958, p. 141-145).

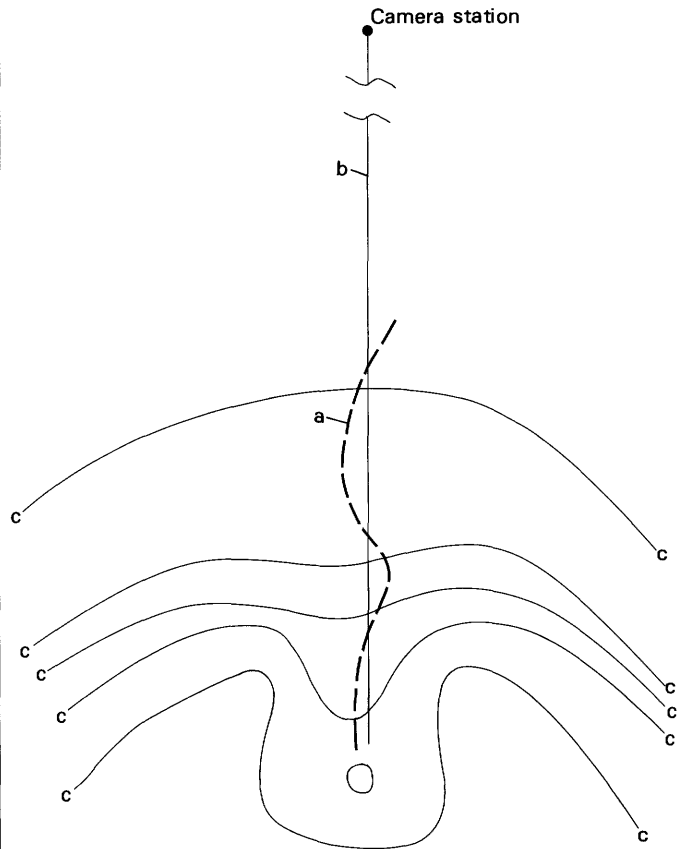


FIGURE 20.—Diagrammatic topographic map illustrating construction of average vertical profile through flow path: a, flow path; b, vertical-projection plane; c, topographic contour lines.

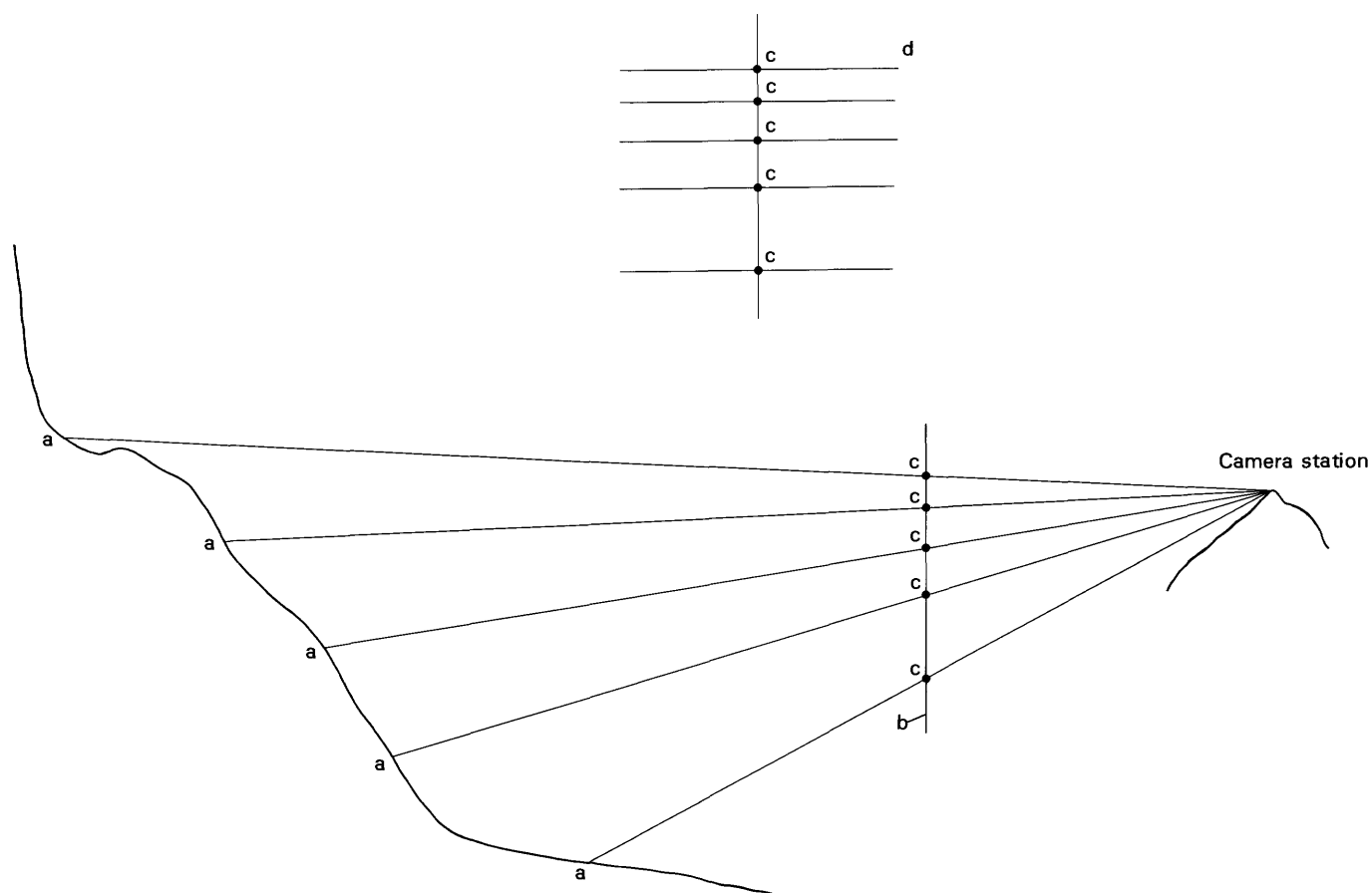


FIGURE 21.—Diagrammatic vertical profile through average flow path: a, topographic contour points used to construct the profile; b, vertical line drawn through rays connecting camera station and topographic contour points; c, intersection points of vertical line and rays (used to construct d); d, overlay showing the spacing between topographic contours traversed by the flow front as seen from the camera station.